

Effect of Casing Material on performance of Cased Munitions



Names: Nauman Sahu

Reg.No:203017

**This thesis is submitted as a partial fulfillment of the requirements for
the degree of**

MS in Energetic Materials Engineering

Supervisor Name: Dr. Abdul Qadeer Malik

School of Chemical and Materials Engineering (SCME)

National University of Sciences and Technology (NUST)

H-12 Islamabad, Pakistan

September, 2019

Dedication

Dedicated to my Beloved Parents, wife and kids

Acknowledgments

All praises to Allah, the Most Gracious and the Most Merciful, the definitive creator of the universe, who bestowed me with strength, consistency and wisdom to complete this research work.

I would like to express my sincere gratitude to my supervisor Dr Abdul Qadeer Malik for the continuous guidance during the research phase. With his sheer dedication and immense knowledge, he was always available to respond my questions and queries. I would also like to thank my GEC members, Dr Muhammad Ahsan, Dr Sara Farrukh and Dr Zaheer Ud Din Babar for their guidance, insightful comments and encouragement. In particular, I am grateful to Dr Muhammad Ahsan, who steered me towards numerical simulation techniques, and provided regular assistance, whenever I got stuck. The thesis would have never been accomplished without his guidance and support.

My special thanks to Dr Aftab Akram, who was very helpful in defining materials for my research work. I am highly grateful to Mr. Khursheed, a fellow PhD student, for his precious support in imparting with basic knowledge/techniques of ANSYS Autodyn. I thank my fellow students Sqn Ldr Muzzamil Ghauri, Sqn Ldr Muhammad Waqas and Muhammad Aftab for all the support and fun we had in last 02 years. My special thanks to Mr. Gulfam and the entire lab staff for their help and support in simulation.

In the end, I would like to thank my family: my parents, wife and kids for their prayers and support. Special thanks to my better half for easing me out at my domestic fronts, and dedicate myself to research work.

Last but not the least; I would like thank Principal Dr. Arshad Hussain, HoD's, all faculty and staff of SCME for providing me all the facilities and administrative support during the research work. In particular, I am highly grateful to Col (Retd) Nadeem Ehsan and Dr Sara Farrukh for their sheer dedication, support and continuous guidance. It has been a very exciting and learning period for me and I will cherish these memories for rest of my life.

Abstract

Prediction of blast parameters for cased munitions always remains prime interest for explosive experts and researchers in the field of energetic materials. These parameters not only assist us in characterization of warhead (warhead design and safety analysis) but are also the direct measure of performance/efficiency of warhead. These blast parameters include initial fragments velocity of fragments, shock wave pressure, number/size of fragments produced and spatial distribution of fragments. Determination of these parameters is a challenging task due to high cost of arena testing (acquisition of firing range and precise equipment like high speed cameras to measure fragments velocities), adhering to the safeties involve in handling of explosives, time and lot of manpower/other resources. Alternatively, numerical simulation techniques can be used to model the blast/fragmentation behavior of cased munitions. Besides providing better understanding of blast/fragmentation phenomena, these softwares can estimate blast parameters of fragmenting warheads. In this study, Autodyn with SPH (Smoothed Particle Hydrodynamics) solver is used to predict the blast parameters of a thick walled cylinder filled with Composition B explosives. Multiple simulations have been carried out by varying casing materials for same warhead. Comparative analysis of different casing materials has been carried on basis of predicted blast parameters of fragmenting warheads. On basis of simulation results, cast ductile iron has been recommended as an alternative casing material to conventional steel casing on basis of its better fragmentation characteristics, high end performance (higher strength, superior shock absorption, corrosion/abrasion resistance etc.) and cost effectiveness. It has been concluded that the casing material also affects the performance of fragmented warheads vis-à-vis efficiency of cased munitions.

Keywords: warhead; fragmentation; blast parameters; Autodyn

Contents

| | |
|---|-----|
| Dedication | i |
| Acknowledgments | ii |
| Abstract | iii |
| List of Figures..... | vii |
| List of Tables..... | ix |
| CHAPTER 1: INTRODUCTION | 1 |
| 1.1 The Detonation Train..... | 1 |
| 1.2 Warhead Characteristics | 2 |
| 1.2.1 Damage Volume | 2 |
| 1.2.2 Attenuation | 2 |
| 1.2.3 Propagation | 3 |
| 1.3 Types of Warheads..... | 3 |
| 1.3.1 Blast Warheads..... | 3 |
| 1.3.2 Fragmentation Warheads..... | 4 |
| 1.3.3 Shaped Charge Warheads | 4 |
| 1.3.4 Continuous-Rod Warheads..... | 4 |
| 1.3.5 Special-Purpose Warheads..... | 5 |
| 1.4 Fragmentation Process of Warhead..... | 6 |
| 1.5 General Purpose Warheads..... | 7 |
| 1.6 Efficiency of Fragmented Warhead | 8 |
| 1.7 Problem Statement | 9 |
| 1.8 Motivation | 9 |
| 1.9 Available Approaches & Proposed Solution | 10 |
| 1.10 Objectives | 10 |

| | |
|---|----|
| CHAPTER 2: LITERATURE REVIEW..... | 12 |
| 2.1 Empirical Formula’s to Determine Blast Parameters | 12 |
| 2.2 Calculation of Blast Parameters Using Simulation Softwares | 14 |
| CHAPTER 3: MODELING AND SIMULATION SETUP | 16 |
| 3.1 Autodyn (SPH Solver)..... | 16 |
| 3.2 Selection of Fragmented Warhead | 17 |
| 3.3 Materials Selection for Warhead | 18 |
| 3.4 Material Properties | 20 |
| 3.5 Equation of State (EOS) for Explosive Fill | 20 |
| 3.6 Modelling of the Warhead and Blast Setup | 22 |
| 3.7 Validation of Simulation Model..... | 24 |
| 3.7.1 Charge to Mass Ratio (C/M) | 26 |
| 3.7.2 Spatial Distribution of Fragments..... | 27 |
| 3.7.3 Fragments Velocities | 27 |
| 3.7.4 Total Fragments Produced | 29 |
| 3.7.5 Final Verdict on Validation of Our Simulation Model | 32 |
| CHAPTER 4: RESULTS AND DISCUSSIONS | 33 |
| 4.1 Expansion and rupture process of Warhead..... | 33 |
| 4.2 Velocity of Fragments..... | 35 |
| 4.2.1 A106 Grade C (Seamless Carbon Steel) | 36 |
| 4.2.2 ASTM A27 Grade 65-35 (Cast Carbon Steel) | 37 |
| 4.2.3 ASTM A536 Grade 60-40-18 (Cast Ductile Iron)..... | 39 |
| 4.2.4 ASTM Grade 40 (Grey Cast Iron) | 41 |
| 4.2.5 ASTM A536 Grade 60-42-10 (Ductile Cast Iron)..... | 42 |
| 4.2.6 Predicted Average Fragments Velocities..... | 44 |

| | | |
|-------|--|----|
| 4.3 | Fragmentation process..... | 45 |
| 4.3.1 | Fragments Mass Distribution | 45 |
| 4.3.2 | Total Number of Fragments Produced | 46 |
| 4.4 | Comparative Analysis of Results..... | 50 |
| 4.5 | Comparison of Physical Properties..... | 51 |
| 4.5.1 | Composition/ Structure | 51 |
| 4.5.2 | Strength | 51 |
| 4.5.3 | Shock Absorption..... | 52 |
| 4.5.4 | Weldability..... | 52 |
| 4.5.5 | Abrasion Resistance..... | 52 |
| 4.5.6 | Corrosion Resistance | 52 |
| 4.6 | Cost Effectiveness..... | 53 |
| 4.7 | Improved Lethality Warhead (ILW) program | 53 |
| | Conclusion | 55 |
| | Recommendations..... | 57 |

List of Figures

| | |
|---|----|
| Figure 1: Functional Components of Warhead..... | 1 |
| Figure 2: High Explosive Detonation Train | 2 |
| Figure 3: Detonation of High Explosive and formation of fragments..... | 6 |
| Figure 4: Low Drag MK-82 GP Bomb (left) and GBU-12 Laser Guided Bomb (right)..... | 7 |
| Figure 5: PK-82 GP Bomb (500 Lbs.)..... | 8 |
| Figure 6: Cylindrical Explosive having Charge mass ‘C’ and shell mass ‘M’ | 13 |
| Figure 7: Schematic diagram of cylinder | 18 |
| Figure 8: 1/4 Computational Model of Warhead..... | 22 |
| Figure 9: Full Scale Model of Warhead | 23 |
| Figure 10: Location of Gauges and Detonation initiation Point on Simulated Warhead | 24 |
| Figure 11: Johnson-Cook parameters for AISI 4340 Steel..... | 25 |
| Figure 12: Total Mass Vs Time for Autodyn Simulation..... | 26 |
| Figure 13: Spatial Distribution of Fragments in Autodyn (left) and in GRIM Software (Right).. | 27 |
| Figure 14: Translation of Angular Zones into Gauge Points..... | 28 |
| Figure 15: Y-Velocity Vs Time for Gauges 5-8..... | 29 |
| Figure 16: Side View of Spatial Distribution of Fragments..... | 30 |
| Figure 17: Mass distribution of fragments | 31 |
| Figure 18: The expansion / rupture process of the cylindrical | 33 |
| Figure 19: Formation of fragments from steel casing at time $t=0.4$ msec..... | 34 |
| Figure 20: Gauges 5 - 8 installed on Warhead Casing | 35 |
| Figure 21: Fragments Velocities vs Time at Gauges 5-8 | 36 |
| Figure 22: Max/Min Values of Fragments Velocities at Gauges 6 and 7 | 37 |
| Figure 23: Fragments Velocities vs Time at Gauges 5-8 for ASTM A106 Gr C..... | 38 |

| | |
|---|----|
| Figure 24: Max/Min Fragments Velocities at Gauges 6-8 for ASTM 27 Gr 65-35 | 39 |
| Figure 25: Fragments Velocities vs Time at Gauges 5-8 for warhead having casing material ASTM A536 Gr 60-40-18 | 40 |
| Figure 26: Max/Min Values of Fragments Velocities at Gauges 6 & 7 for A536 Gr 60-40-18.... | 41 |
| Figure 27: Fragments Velocities vs Time at Gauges 5-8 for casing material ASTM Grade 40.... | 42 |
| Figure 28: Max/Min Values of Fragments Velocities at Gauges 6 & 7 for ASTM Gr 40 | 42 |
| Figure 29: Fragments Velocities vs Time at Gauges 5-8 for warhead having casing material ASTM A536 Gr 60-42-10 | 43 |
| Figure 30: Max/Min Values of Fragments Velocities at Gauges 6 & 7 for A536 Gr 60-42-10.... | 44 |
| Figure 31: Predicted Average Fragments Velocity (Autodyn) for all Warheads | 44 |
| Figure 32: Fragments Mass Distribution for ASTM A106 Grade C | 45 |
| Figure 33: Predicted Total Number of Fragments (Autodyn) for all warhead casings | 47 |
| Figure 34: Extract from Fragments Analysis Report of Casing Material A106..... | 47 |
| Figure 35: Extract from Fragments Analysis Report of Casing Material ASTM A27..... | 48 |
| Figure 36: Extract from Fragments Analysis Report of Casing Material A536 Grade 60-40-18 . | 48 |
| Figure 37: Extract from Fragments Analysis Report of Casing Material ASTM Grade 40..... | 49 |
| Figure 38: Extract from Fragments Analysis Report of Casing Material A536 Gr 60-42-10 | 49 |

List of Tables

| | |
|--|----|
| Table 1: A106 Grade C Chemical Composition*..... | 19 |
| Table 2: A106 Grade C Mechanical Properties*..... | 19 |
| Table 3: Selected Materials for Comparative Analysis & their Mechanical Properties*..... | 19 |
| Table 4: Properties of Selected Materials for defining in Autodyn..... | 20 |
| Table 5: JWL constants for Comp B Explosive | 21 |
| Table 6: Comparison of Physical Parameters Simulation/Experimental Model | 25 |
| Table 7: Comparison of Initial Fragments Velocities | 29 |
| Table 8: Comparison of Fragments produced during experiment/simulation | 31 |
| Table 9: Summary of Fragmentation Analysis Report for Different Warheads..... | 46 |
| Table 10: Comparative Analysis of Total Number of Fragments Produced | 50 |
| Table 11: Comparison of Strength between Cast Ductile Iron vs Cast Steel | 52 |
| Table 12: Cost Comparison between Cast Ductile Iron Vs Cast Carbon steel..... | 53 |

CHAPTER 1: INTRODUCTION

A warhead is most important component of the weapon having destructive capability. It may be an explosive or toxic material that is delivered by a missile, precision guided munition (PGMs), rocket, or torpedo. Traditional warheads use blast or fragmentation effects to damage the target. The standard warhead comprises of three main functional parts [1] as shown in Figure 1:

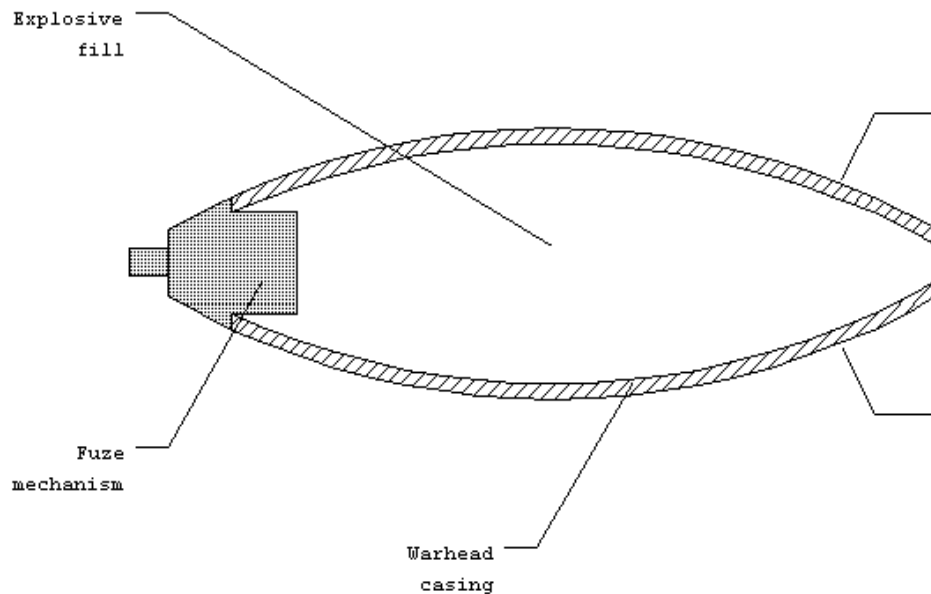


Figure 1: Functional Components of Warhead

1.1 The Detonation Train

The detonation train or triggering sequence is sequence of events to initiate warhead. The detonation train comprises a detonator (primary explosive); booster charge (secondary explosive) and main charge (high explosive) as shown in Fig 2. The sequence of operation will be from left to right in figure 1. First of all, detonator is initiated by electrical spark or mechanical shock. The output from detonator is low powered but enough to reliably initiate the secondary explosives (booster charge). Subsequently, the detonation of the booster charge will results in a shock wave of sufficient strength to initiate the main charge. The sensitivity of components used in

detonation train decreases from left to right. Primary explosive are more sensitivity (i.e. can easily initiated) and are used in small quantities in relatively safely packaged forms. Due to their high sensitivity, initiator charges or detonators require special care during storage and handling. Booster charges are less sensitive than detonators but more sensitive as compared to main charge, which is highly insensitive.

All the components of detonation train (i.e., detonator, booster and main charge) are never stored in assembled form to avoid accidental initiation. They are rather stored independently and are assembled up prior to mission requirement.

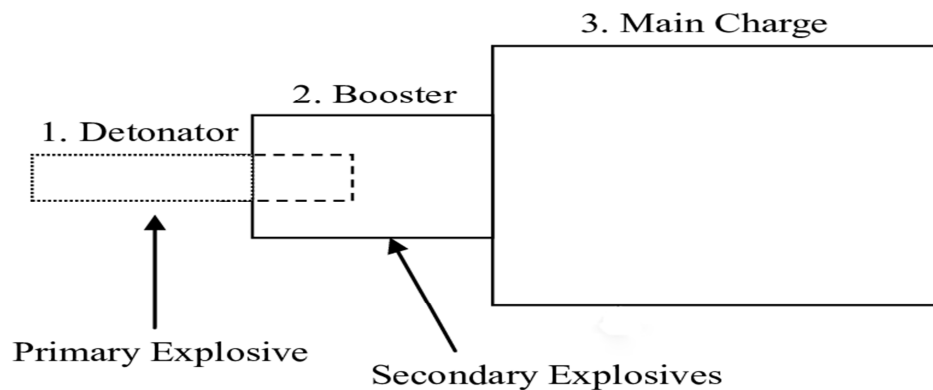


Figure 2: High Explosive Detonation Train

1.2 Warhead Characteristics

Being the most important component of the weapon, warhead achieves its desired objectives by effectively damaging the target. The damage to the target can be assessed on following parameters [1]:

1.2.1 Damage Volume The warhead is considered to be enclosed in an envelope that sweeps along the flight path of the target (aircraft/missile). The volume of this envelope will define the limit of destruction of the payload.

1.2.2 Attenuation Attenuation is gradual decrease of blast intensity away from the explosion source. As blast wave/fragments travels away from the point of origin; its destructive power keep decreasing continuously until it is totally harmless.

1.2.3 Propagation After detonation, the way in which blast wave and fragments are dispersed from payload is called propagation. When the propagation of a warhead is uniform in all directions, it is called isotropic. If it's not uniform, it is called non-isotropic.

1.3 Types of Warheads

The killing performance of a fragmented warhead is of great interest in modern warfare. On basis of their role and type of damage they impart, Warheads are classified into five categories [1]:

- Blast Warheads
- Fragmentation Warheads
- Shape charges
- Continuous rod Warheads
- Special-purpose Warheads

1.3.1 Blast Warheads A blast warhead achieves destruction of the target primarily by blast effect. When a cased munition detonates, the inside temperature and pressure will increase rapidly and the casing starts to expand until it breaks up into fragments. After the blast, due to compression of the surrounding air, the pressure and temperature rises from atmospheric values to peak overpressure in a fraction of a micro second. For a typical high explosives warhead, the initial values of pressure and temperature are 200 kilo bars and 5,000°C respectively. Due to sudden rise of temperature and pressure, shock wave is formed. After some time, the temperature and pressure will reduce to atmospheric values. This phase of shockwave is known as the positive phase. The pressure will keep on reducing to sub-atmospheric pressure and subsequently returns to the normal values. This will form the negative (or suction phase) of the shockwave. This positive/negative pressure variation will create a push-pull effect on target, and cause the target to collapse due to internal pressure.

1.3.2 Fragmentation Warheads A fragmentation warhead is designed to damage the target by the high velocity fragments produced due to bursting of the warhead casing. After the fragmentation process has initiated, the blast energy (approximate 30%) will be imparted to fragments in form of kinetic energy [1]. The fragmentation process of cased munition is dependent upon charge-to-mass ratio (C/M), the material properties of casing, and the explosive power of filler charge [2]. While, the number of fragments produced, Size and propagation of fragments and fragments velocities are direct measure of warhead efficiency [3]. Higher the number of fragments and initial velocities more will be the damage imparted to the target.

1.3.3 Shaped Charge Warheads Shaped charges are designed to concentrate the effect of the explosive's energy in specific direction. A conventional shaped charge comprises a charge casing, a hollow liner of metal, and a high explosive fill between the liner and case. Once high explosive is detonated, the detonation wave collapse the metal liner and it get ejected in the form high velocity jet. The velocity at forward tip of jet is as fast as 10 km/sec [4]. Having high velocity and extreme pressure, the jet perforates the target material. The performance of shaped charge is dependent upon type of explosive fill, charge shape and powdered metal lining. The shaped charges are used to cut or form metals, penetrate armor, and perforate well in oil and gas industry.

1.3.4 Continuous-Rod Warheads A continuous-rod warhead comprises a long rods arranged in a circular bundle around the main explosive charge. Once it explodes, the rods spread into a large circle that cuts the target. These warheads are effective in anti-aircraft and anti-missile role. Upon detonations, these rods can attain maximum velocities from 1050 to 1150 m/sec [1]. However, in modern fragmenting warheads, the initial fragment velocities are ranging between 1800 to 2100 m/sec. Due to this reason; the continuous-rod warheads are being replaced with blast/fragmentation warheads in latest anti-aircraft missiles.

1.3.5 Special-Purpose Warheads Special purpose warheads are specialized weapons designed to perform a specific. Some examples of special-purpose weapons are as follows:-

- ***Thermal Warheads*** Some targets are effectively destroyed by fire power. For such targets, thermal warheads are used. Thermal warheads use chemical energy to kindle fires e.g. incendiary or fire bombs.
- ***Biological and Chemical Warheads*** These warhead uses infectious agents, such as anthrax spores or other biological agents for causing sickness or death to humans. These warheads have an extreme strategic importance as they causes temporary disability to personnel thus making it more convenient to capture or neutralize an enemy installation without damaging buildings or materials. An explosive charge is placed in a biological warhead for rapid dispersion of biological agents.
- ***Pyrotechnic Warheads*** Pyrotechnics refers to produce fire through chemical reaction with goal to produce light, heat, noise and pressure. These warheads are usually employed for signaling, illuminating, ejection seat operation and marking targets.
- ***Cluster Bomb Units (CBU)*** CBUs are primarily used for area denial purposes. Hundreds of CBUs are packed in a canister that is dispersed in air after drop from the aircraft. Each of these bomblets is programmed (for several hours) to explode at specific time thus denying the area for extended hours. These warheads provide a wide area of coverage and are effective against armored vehicles, personnel and other soft targets.
- ***Mines*** A landmine is an explosive device, buried under or on the ground and is used to destroy or neutralize enemy targets, ranging from troops to armored vehicles, tanks when they pass over it or close by. These devices are normally triggered automatically due to pressure applied on them by target walking over it or in close proximity.

1.4 Fragmentation Process of Warhead

As the research title indicates, our focus during this study will remain on cased munitions (i.e. explosive charge is enclosed in a metallic casing) having blast (overpressure) waves and fragmentation effects to destroy the target [5]. When this type of warhead detonates, due to decomposition of explosive, there is sudden increase in pressure and temperature inside the casing. Due to this high pressure, the casing starts to expand until it breaks up into number of high-velocity fragments [6]. The fragmentation process of cased munitions is normally governed by charge-to-mass ratio (C/M), properties of casing material, and the explosive power of filler charge [2]. While, the blast parameters like Number and size of fragments produced, spatial distribution of fragments and initial fragments velocities are direct measure of warhead efficiency [3]. Therefore, to improve the efficiency of fragmenting warheads, we either need to increase fragment velocities or to eject more fragments in target direction [7]. Higher the number of fragments produced, more will be the probability of warhead to neutralize the target. Similarly, higher the fragments initial velocities, the more will be the range of fragments and penetration into the target. Figure 3 shows a detonation of fragmented warhead.



Figure 3: Detonation of High Explosive and formation of fragments

1.5 General Purpose Warheads

General Purpose Warheads are typical example of cased munitions. GP (General Purpose) bombs are being used extensively around the world since 1950's. These are air delivered munitions designed to destroy the ground targets with blast and fragmentation effects. The designation 'General Purpose' in description of the bomb indicates that GP Bombs are flexible weapons and can be deployed against variety of targets such as concrete piercing (buildings/ installations), runway cratering and anti-personnel role through blast and fragmentation effects.

The Mk-82 is 500 Lbs. (227 kg) GP Bomb containing 87-89 kg of high explosive in a forged steel body having weight of 140-142 kg. It is the steel casing that creates the primary fragmentation for the bomb. The propagation and size of fragment is random and dependent upon the shape of warhead. The dispersal pattern and size of the fragments is largely random. Initially, these bombs were delivered unguided with accuracy of 5.5% to hit the target as [8]. Guided versions of GP Bombs also known as PGMs (Precision Guided Munitions), have high accuracy and are used for precision strikes. During the Operation Desert Storm in 1991, 88% of the dropped GBU-12 successfully hit its targets [8]. Figure 4 shows the MK-82 GP Bomb (left) in standard configuration, while GBU-12 Laser Guided Bomb (right).

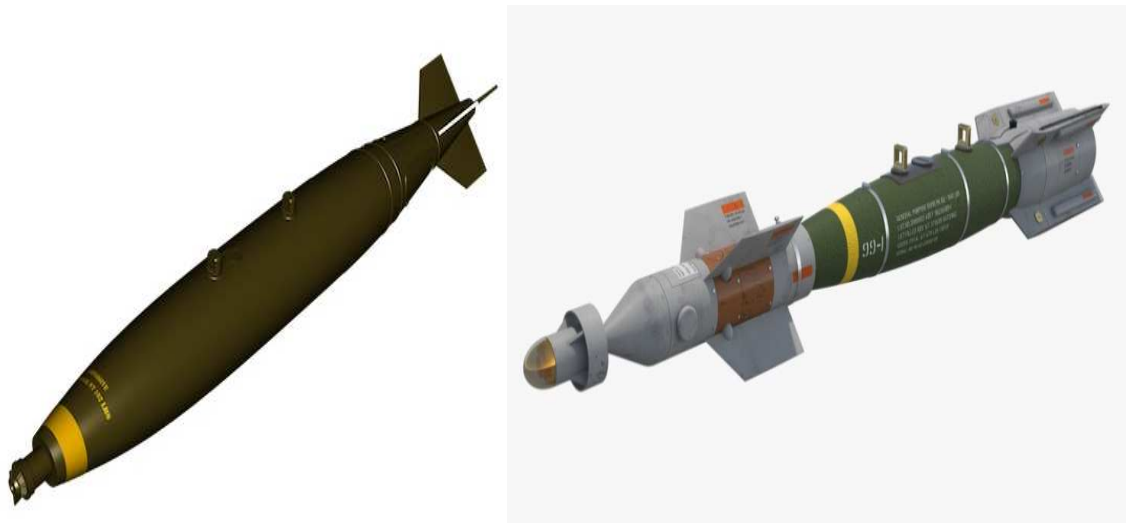


Figure 4: Low Drag MK-82 GP Bomb (left) and GBU-12 Laser Guided Bomb (right)

PK-82 is the Pakistani Variant of MK-82 bomb being produced by Pakistan Ordnance Factories (POF), Wah Cantt, using Composition 'B' as explosive fill and Carbon Steel (ASTM A106 Grade 'C') as casing material. This warhead is being produced since 1980's, with same explosive fill and the casing material. Figure 5 shows the PK-82 GP Bomb being manufactured by POF, Wah Cantt.



Figure 5: PK-82 GP Bomb (500 Lbs.)

1.6 Efficiency of Fragmented Warhead

The efficiency of the warhead generally depends upon the total kinetic energy of the fragments generated after the blast. To obtain a high kinetic energy, it is essential to maximize the speed or mass of the fragments. However, higher mass of fragments will reduce the number of fragments. For this reason, the best solution for designing fragmented warheads is to maintain a balance between number and size of fragments produced.

The blast parameters like Number and Size of fragments produced, spatial distribution of fragments and initial fragments velocities are direct measure of warhead efficiency [6]. Therefore, to improve the efficiency of fragmenting warheads, we either need to increase fragment velocities or to eject more fragments in target direction.

The improvement in efficiency of the existing PK-82 GP Bomb can be achieved by changing design, filler explosive or Casing material. Changing design of existing warhead is like designing a new warhead which will be subsequently subjected to long and tiresome process of qualification and arena testing. Similarly, change of explosive fill is also dependent on existing explosive filling setups and acquiring a new filling

setup is not a cost effective solution. However, with the advancements in the field of material sciences, a significant improvement in efficiency of warhead can be achieved by selecting suitable casing material.

1.7 Problem Statement

The problem statement for this research is to improve the efficiency of cased munitions like PK-82 GP bomb by selecting a suitable casing material.

The main purpose of looking for alternative material is to enhance the efficiency of warhead by selecting suitable casing material. The alternate material will be finalized on basis of better fragmentation characteristics (i.e. to increase fragment velocities or to eject more fragments in target direction) and having excellent physical properties.

1.8 Motivation

The main motivation behind the study is to improve efficiency of PK-82 GP Bomb, which is being used by PAF since 1980's, without any modification or improvement.

Similar type of study has been initiated in 2015 by Unites States Department of Defense (DoD) to improve the fragmentation characteristics of existing GP bombs. Obviously, we will not be shared with the outcome of this research.

Being a restrictive field, limited literature is available in the field of energetic materials. Moreover, latest developments in this field are considered trade secrets by the manufacturers.

Last but not the least, the study will be helpful for local industry in Pakistan and will provide them an opportunity to go for alternate casing material for PK-82 GP Bombs. Besides improving efficiency of warheads, alternate casing might also provide a cost effective solution.

1.9 Available Approaches & Proposed Solution

An explosion of high explosive projectiles is highly non-linear transient phenomena as it will be followed by shock, explosion and fragmentation effects. Therefore, various physical processes must be taken into account to accurately characterize such events.

Presently, following three approaches are being used to understand blast/fragmentation behavior of warheads.

- Firstly, empirical formulas can be used to solve simplest and highly idealized problems.
- Second option is to use analytical techniques (based on numerical softwares) to predict fragmentation behavior and blast parameters. But these analytical techniques are based on available experimental data and can solve limited range of problems.
- Third and most reliable approach to handle blast/fragmentation is physical experiments. However, these experiments can be very costly and often difficult for instrumentation, acquisition and interpretation of results.

Due to development of numerical softwares and availability of more powerful computers, it is now possible to investigate the blast and fragmentation analysis of warhead. Numerical simulation softwares have enabled us to model a blast/fragmentation process of cased munitions and to predict blast parameters vis-a-vis warhead efficiency. In this study, ANSYS Autodyn software is used for numerical simulations, which is an excellent tool to model fragmentation process of cased munitions.

1.10 Objectives

Following objectives were defined to achieve the desired goal:-

- To model different warheads with varying casing material in ANSYS Autodyn.
- To predict blast parameters by subjecting each warhead to blast simulation using SPH solver technique.
- To perform the comparative analysis of predicted blast parameters and to recommend suitable casing material for cased warhead.

CHAPTER 2: LITERATURE REVIEW

An explosion of highly explosive projectiles is always followed by shock, explosion and fragmentation, and reaction problems involve highly non-linear transient phenomena. Therefore, various physical processes must be taken into account to accurately characterize such events. Physical experiments combined with analytical techniques are required to understand full physics. Presently, following three approaches are being used to understand blast/fragmentation behavior of warheads. Firstly, empirical formulas can be used to solve simplest and highly idealized problems. Second option is to use analytical techniques (based on numerical softwares) to predict fragmentation behavior and blast parameters. But these analytical techniques are based on available experimental data and can solve limited range of problems. Third and most reliable approach to handle blast/fragmentation is physical experiments. However, these experiments can be very costly and often difficult for instrumentation, acquisition and interpretation of results.

2.1 Empirical Formula's to Determine Blast Parameters

In 1943, R. W. Gurney [9] derived a simple analytical equations to determine the initial velocity of fragments from an exploding warhead. As per this model, the initial fragments velocities could be estimated by Charge to Mass ratio (C/M) of warhead, where C is the mass of explosive fill or charge and M is the mass of casing, as shown in Figure 6. The Gurney's equation to calculate initial velocity of fragments for cylindrical warhead is as follows:-

$$\frac{v}{\sqrt{2E}} = \left(\frac{M}{C} + \frac{1}{2} \right)^{-\frac{1}{2}}$$

Where,

V= Fragments Velocity,

M = Mass of casing,

C= mass of Explosive fill,

$$\sqrt{2E} = \frac{D}{2.97} = \text{Constant (2.79 to 3.15 for typical military explosives),}$$

D = Detonation Velocity

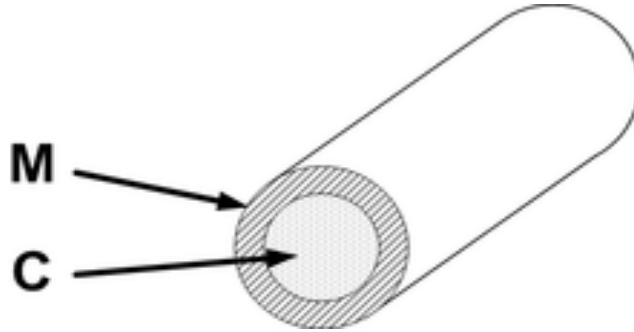


Figure 6: Cylindrical Explosive having Charge mass 'C' and shell mass 'M'

The Gurney's equation was simple and reasonably accurate to undertake manual calculations of initial fragments velocity. However, later studies revealed shortcomings in Gurney's formula that it doesn't cater material properties of casing (i.e., tensile/yield strength and failure strain), which otherwise plays a significant role in fragmentation [10]. Using Gurney's model, U. Fano [11] compared blast of cased charge with bare charge explosive on basis of kinetic energy. He developed an equation to calculate the kinetic energy of blast gases after energy portioning with the casing. E. M. Fisher [12] found disparities in blast pressure and impulse calculated by Fano's equation with experimental data, which he acquired by performing series of experiments. On basis of his comparison, he suggested improvements in Fano's equation. As compared to Gurney's model, Fisher's approach was more consistent with experimental data, but it departs from Gurney's basic assumption of uniform gas pressure etc.

Mott [13] presented a fragmentation model for break-up of cylindrical warhead to predict the number of fractures and mass of fragments produced. As per this model [14], "the average length of the circumferential fragments is a function of the radius and velocity of the ring at the moment of break-up, and the mechanical properties of the

metal". The model paved the way for further research and is still valid to explain fragmentation pattern of ductile materials.

John Pearson [2] explained the behavioral process of fragmented warhead from expansion to fracture and fragmentation respectively. As per this model, the fragmentation process was divided into four phases:

- the case behaves elastic-plastic
- expansion of the case continues till fractures start to develop
- start of the fragmentation process
- each fragment achieves initial velocity and start moving towards target

Grady and Hightower [15] developed a model based on energy/momentum conservation in fragmentation process and derived an equation to predict circumferential fractures spacing. Arnold and Rottenkolber [16] investigated fragmentation behavior of warhead casings of varying thickness. Fragments mass distribution of 04 exploding shells was determined and it was concluded that that material properties lay an important role in fragmentation process. Hutchinson [17-20] suggested improvements in Gurney's equations [9] and presented new and improved theoretical formulas based on impulse and momentum analysis for cased munitions.

Zecevic etal [21] investigated the effects of material properties of casing on the initial fragments velocities and spray angles of fragments. On basis of experimental data, he developed a relationship for selection of an optimum warhead casing material. He concluded that higher the R_m/R_v (ratio of tensile strength to yield strength of casing material), more will be the number of fragments produced.

2.2 Calculation of Blast Parameters Using Simulation Softwares

Due to development of numerical softwares and availability of more powerful computers, it is now possible to investigate the fragmentation analysis of fragmenting warheads. These softwares not only allow to model a simple geometric shaped warheads but complex design warheads can be imported from specific softwares designed for creating drawings/models. These softwares are able to handle wider range of problems

and assist us to understand full physics of the blast phenomena. Moreover, these numerical techniques offer effective solutions by avoiding financial resources and time of physical experiments. Additionally, these tools are able to predict even those parameters, which are difficult to be measured from physical experiments [22].

Anderson et al. [23] predicted the final velocities of fragments by modelling a cylindrical warhead using a two-dimensional finite-difference code and showed that predicted values are in good agreement to experimental values. Using simulation software “PAFRAG” based on three-dimensional axisymmetric hydrocode, Gold et al. [24] predicted the performance of cased munitions and validated the simulation results with existing experimental data. Kong Xiangshao et al. [25] successfully demonstrated the capabilities of Autodyn SPH solver to simulate fragmented warheads. He was able to predict all the blast parameters. Upon comparison, the simulation results show close approximations with the experimental results. I.G. Cullis et al. [26] examined the blast and fragmentation process of cylindrical warhead (thick-walled) using Eulerian hydro code based numerical software “GRIM”. He was able to predict the spatial distribution of fragments, initial fragments velocities and the total number of fragments produced during the fragmentation process. He compared the simulation results with the experimental results by subjecting similar charge to detonation. The predicted values were observed in close approximation to experimental values.

G. Tanapornraweevit [10] conducted numerical studies of the fragmentation process of cased warhead while focusing on effect of material properties of casing material on fragmentation process. He concluded that initial yield strength and ultimate strength of casing material has minimal effects on the initial fragments velocities and spray angles of fragments. Moreover, a warhead having brittle casing material with low failure strain will produce more fragments with low average fragment mass.

CHAPTER 3: MODELING AND SIMULATION SETUP

To determine blast parameters of the fragmented warheads, experimentation is considered as best and reliable tool around the world. However, it is difficult to draw general conclusions on basis of experiments only, due to variation in results. The variations in results normally occur due to different apparatus/test equipment, variation in test setup and varying atmospheric conditions, general skill and operator's proficiency etc. Furthermore, experimental testing of explosives is very costly and time consuming activity. Numerical simulations are mostly used to study blast/fragmentation process and to predict blast parameters. They enable great savings in terms of costs and man-hours required for physical experiments and make it possible to predict blast parameters which are virtually impossible to measure in physical experiments can be examined in detail. However, these numerical simulations can never substitute experiments, and should be used in combination with experiments to validate numerical models.

3.1 Autodyn (SPH Solver)

ANSYS Autodyn is a versatile explicit analysis tool for modeling the non-linear dynamics of solids, fluids, gases and their interactions. This software assists us in designing/modelling of warheads and test setup, followed by their initiation to investigate the blast and fragmentation behavior of warhead. Autodyn comprises of four different solver techniques:-

- Finite element (FE) solvers for computational structural dynamics
- Finite volume solvers for Computational Fluid Dynamics (CFD)
- Mesh-free/particle methods for large deformation and fragmentation
- Multi-solver coupling for multi-physics solutions

Each solver has a capability to address specific type of problem. For e.g. SPH-Lagrange solvers can be used for nonlinear dynamic problems i.e., hyper velocity

impacts and failure of brittle materials by explosion and SPH solver is used to undertake blast / fragmentation simulation [22].

In this study, Autodyn SPH solver has been used to investigate blast/fragmentation behavior of thick-walled cylindrical warheads. The SPH solver is a grid less Lagrangian hydrodynamics technique in which the object under study is discretized into a finite set of observation points or small evenly sized particles. The main advantage of SPH over other techniques is that it can also solve the problems with large deformations. The other techniques like Lagrange method face computational termination problem due to large distortion of elements [25]. Similarly, identification of produced fragments is very difficult in Eulerian mesh due to the presence of multi-material 'mixed' cells [26].

At present, the SPH technique is considered best for explaining blast/fragmentation process and prediction of blast parameters of fragmenting warheads. This technique not only predict blast parameters like shock wave pressure, initial fragments velocity etc. but also provides detail fragmentation analysis of casing material by identifying each individual fragment as separate identity [22].

3.2 Selection of Fragmented Warhead

To undertake comparative analysis of blast parameters of fragmented warhead, the first thing we need to select a warhead for numerical investigation. The warhead should contain high explosive and enclosed in metallic casing to produce the fragmentation. Keeping in view these consideration, a thick-walled cylinder warhead mentioned in [26] has been chosen for modelling in Autodyn, as shown in Fig 7. The cylinder has total length of 404 mm. It has inner diameter of 150 mm and the outer diameter is 170 mm. The casing thickness is 65mm at both ends of the cylinder, while thickness of casing at radial portion is 10mm. As the thickness of casing at both ends of cylinder is more than the thickness at radial portion (more than three times), therefore radial portion will produce more fragments of small sizes while both ends will produce less fragments of massive size. The red dot depicted in Fig 3 is the initiator or detonator

to initiate detonation in cylindrical warhead. From here on, the cylinder end where initiation is started will be referred as “near end” and the opposite end of the cylinder will be referred as “far end”.

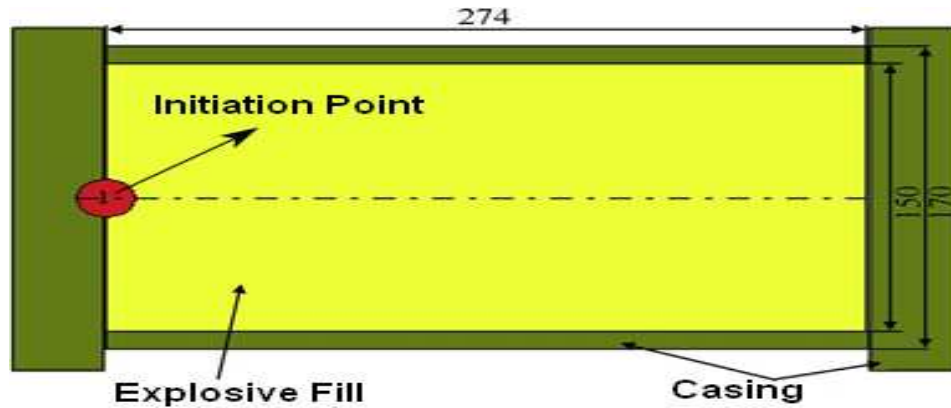


Figure 7: Schematic diagram of cylinder

3.3 Materials Selection for Warhead

Iron is the fourth most common element found in Earth's crust. It is one of the strongest, highly versatile and cheapest metals. It was a back bone of industrial revolution in 17th & 18th century. Pure iron is too soft and highly reactive material and is of not much use. So, it is mostly in the form of iron alloys i.e., iron mixed with other elements (especially carbon) to make it stronger, tougher and resilient. One example of Iron alloy with Carbon is steel, which is being used around the world in various industries like automobile, construction, ship manufacturing, automobiles and defense [27]. Due its higher density, excellent mechanical properties and low cost, alloys of iron are best choice for production of cased munitions like GP bombs. Higher density will add more mass thus will increase the lethality of fragments produced from metallic casing.

As already mentioned in para 1.3 above, that A106 Grade ‘C’ is being used as casing material for PK-82 GP Bomb. Therefore, it will be used as a reference material in comparative analysis of different warhead casings. The main aim of this study is to look for a better alternative to existing casing material i.e. ASTM A106 Grade ‘C’, having better fragmentation characteristics and improved physical properties. The chemical

composition and the mechanical properties of A106 Grade ‘C’ are depicted in Table 1 and 2 respectively:-

Table 1: A106 Grade C Chemical Composition*

| Chemical Composition (%) | | | | | | | | | |
|---------------------------------|-----------|---------|---------|---------|---------|---------|--------|--------|--------|
| C(Max) | Mn | Si(Min) | Cu(Max) | Ni(Max) | Cr(Max) | Mo(Max) | V(Max) | P(Max) | S(Max) |
| 0.35 | 0.29~1.06 | 0.1 | 0.4 | 0.4 | 0.4 | 0.15 | 0.08 | 0.035 | 0.035 |

(*Source: <https://www.makeitfrom.com/material-group/Iron-Alloy>)

Table 2: A106 Grade C Mechanical Properties*

| Mechanical Properties | | |
|------------------------------|------------------------------|----------------------------|
| Grade | Tensile Strength (Mpa), Min. | Yield Strength (Mpa), Min. |
| A106 Grade C | 485 | 275 |

(*Source: <https://www.makeitfrom.com/material-group/Iron-Alloy>)

Different Iron alloys were considered in numerical simulations to find a better replacement to ASTM A106 Grade C. The alternate materials were selected from different categories of iron alloys with varying mechanical properties. The selected materials are depicted in table 3 along with their mechanical properties:-

Table 3: Selected Materials for Comparative Analysis & their Mechanical Properties*

| Material | Category | Tensile Strength (MPa), Min. | Yield Strength (MPa), Min. |
|--------------------|-----------------------|------------------------------|----------------------------|
| A106 Grade C | Seamless Carbon Steel | 485 | 275 |
| AISI 4340 | Steel Alloy | 690 | 470 |
| ASTM 40 | Grey Cast Iron | 310 | 200 |
| ASTM A27 G65-35 | Cast Carbon Steel | 500 | 270 |
| ASTM A536 60-40-18 | Cast Ductile Iron | 460 | 310 |
| ASTM 60-42-10 | | 470 | 320 |

(*Source: <https://www.makeitfrom.com/material-group/Iron-Alloy>)

All the selected materials except ASTM 40 (Grey cast Iron) have higher Tensile strength and Yield strength than the reference material i.e., ASTM A106 Grade C.

Beside other iron alloys, Steel Alloy AISI 4340 (an American equivalent material to EN24W steel) used for thick-walled cylinder warhead mentioned in [26] was also considered for fragmentation analysis. The simulation results of warhead modelled using AISI 4340 (having PBXN-109 explosive) will be used to compare/validate the simulation model with experimental results mentioned in [26].

3.4 Material Properties

Prior to undertake simulations, the selected materials are needed to be defined in Autodyn. Although, there is material library available in Autodyn, but it doesn't encompass all the materials. The material properties used for defining selected materials in Autodyn are appended below in Table 4:-

Table 4: Properties of Selected Materials for defining in Autodyn

| Material | Material Properties | | | | | |
|-----------------------|---------------------------------|---------------------------|------------------|-----------------------------|--------------------------|---|
| | Density (g/cm ³) | Shear Modulus (GPa) | Poisson Ratio | Young's Modulus (GPa) | Bulk Modulus (GPa) | Specific Heat at 20°C (J/Kg.k) |
| A106 Grade C | 7.85 | 79.69 | 0.29 | 203.8 | 161.76 | 470 |
| AISI 4340 | 7.8 | 73 | 0.29 | 190 | 151 | 470 |
| ASTM 40 | 7.5 | 69.77 | 0.29 | 180 | 143 | 490 |
| ASTM A27 G65-35 | 7.8 | 73.64 | 0.29 | 190 | 150.8 | 470 |
| ASTM A536 60-40-18 | 7.15 | 66.02 | 0.28 | 170 | 128 | 461 |
| ASTM 80-60- 03 | 7.5 | 70 | 0.29 | 180 | 143 | 490 |

(Source: <https://www.makeitfrom.com/material-group/Iron-Alloy>)

3.5 Equation of State (EOS) for Explosive Fill

The equation of state (EOS) of detonation products is used to define energetic characteristics of an explosive in numerical simulations softwares. EOS parameters for high explosives are generally determined by performing cylinder tests, in which the motion of the walls of a copper cylinder filled with explosive is measured [28].

Nowadays, the JWL EOS is widely used in practical engineering application and same is appended below:-

$$P_s = Ae^{-R_1v} + Be^{-R_2v} + Cv^{-(1+w)}$$

Where A, B, C, R1, R2, ω are the parameters calculated on basis of cylinder test, while V refers to relative volume.

Pakistan Ordnance Factory (POF), Wah Cantt and Pakistan Air Force (PAF) Munitions Filling Plant, Malir Cantt, both are using Composition 'B' (Comp B) as filling explosive for GP Bombs. Keeping in view the capabilities of existing filling setups, Composition 'B' has been used as a filling explosive in this study.

Composition 'B' is cast able, high explosive formulation of RDX (Cyclonite) and TNT in the proportion 60:40 and also contains wax as an additive in some formulations. It has a density of about 1.717 g/cm³ and detonation velocity of 7980m/s approx. It was developed to replace pure TNT, which was being used as high explosive filler charge for warheads. Due to low melting temperature of TNT (i.e., 80°C approx.), it is easy to cast and fill Comp B in warheads of varying sizes and shapes, e.g. mortars, land mines and air-dropped bombs etc. However, due to its higher sensitivity and chances of accidental initiation by fire or projectile impact, it is replaced by less sensitive cast-able Composition H-6 in many weapon systems [29]. Despite the fact that Comp B has been replaced by less sensitive Composition H-6 it is still being used as an explosive fill for large munitions like GP Bombs. Comp B explosive already exists in material database of Autodyn software and it has been defined there using standard JWL equation of state (EOS). The JWL constants used for Comp B are shown in Table 5.

Table 5: JWL constants for Comp B Explosive

| Density kg/m ³ | A (Pa) | B (Pa) | Ω | R1 | R2 | CJ Energy / Unit Volume (KJ/m ³) | VOD (m/sec) |
|------------------------------|-----------|---------|----------|-----|-----|---|----------------|
| 1660 | 5.2423e11 | 7.678e9 | 0.34 | 4.2 | 1.1 | 8.5e6 | 7980 |

3.6 Modelling of the Warhead and Blast Setup

As Autodyn SPH solver technique was chosen for simulations, therefore the first step was to create a selected warhead [26] as SPH part. Due to symmetrical shape of cylindrical warhead, only a quarter portion of warhead was modelled in Autodyn as shown in Fig 8. In this figure, the green color representing the warhead casing while the blue color representing the explosive fill i.e., Comp B.

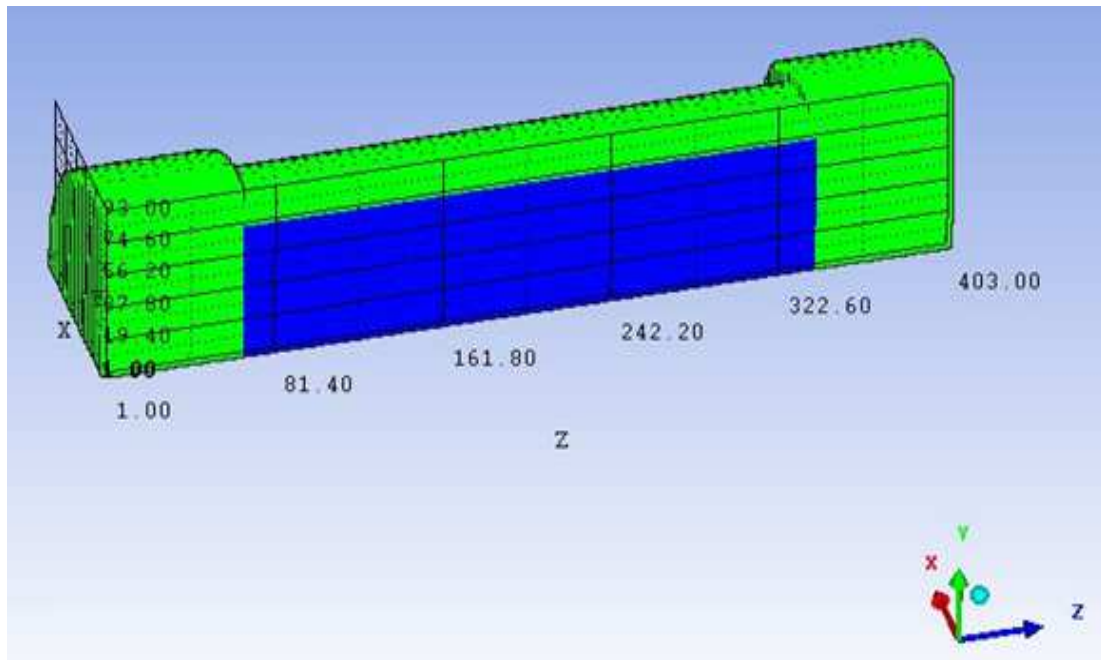


Figure 8: 1/4 Computational Model of Warhead

The creation of quarter model will not only reduce the model size but will also lessen the simulation time as less computational power will be required. However, the results of quarter model can be applied on full scale warhead by using symmetry option in two axes i.e., X-Axis and Y-Axis, as shown in Fig 9.

In SPH solver, both cylindrical casing and explosive fill inside the casing are discretized into number of small evenly sized particles. For an appropriate fragment mass distribution, the particle size should be as small as possible. However, smaller particle size corresponds to large number of particles, which will therefore enhance the simulation processing time. Therefore, we need to maintain a balance between particle size and simulation processing time. During the study, different particle sizes were tried

and the particle size of 2 mm was chosen as it produced 1,56,435 particles of warhead casing, which is considered sufficient to explain the total count of fragments produced in fragmentation process of casing.

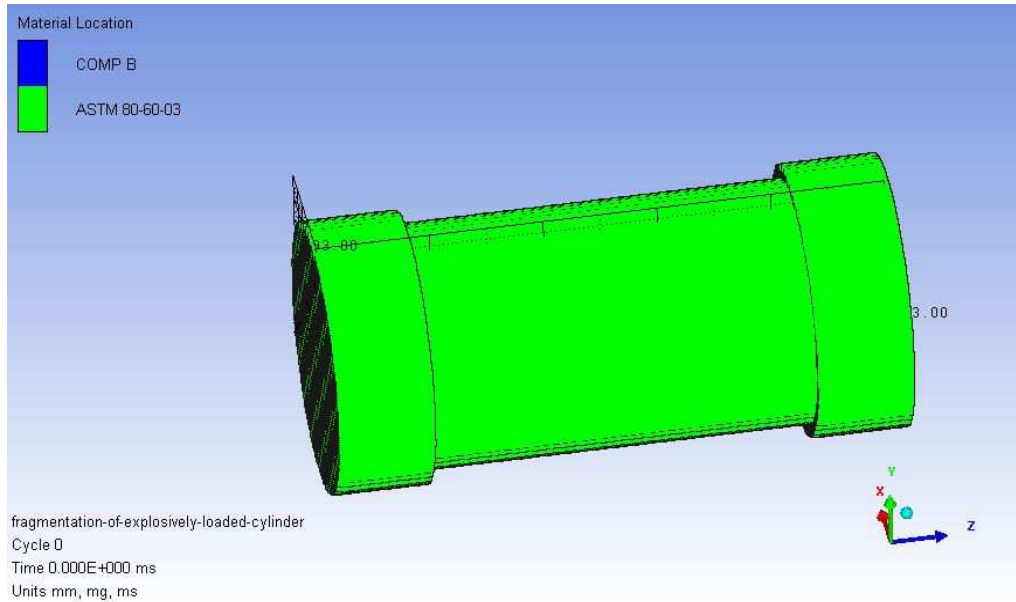


Figure 9: Full Scale Model of Warhead

Beside 2 mm SPH particle size, simulation was also attempted with 1mm and 3 mm SPH particle size. With 1 mm particle size, a total of 1,265,412 particles were formed by warhead casing and simulation process failed to complete despite 2-3 days processing on ordinary laptop. Whereas, with 3mm particle size, a total of 45,374 particles were formed by warhead casing and simulation process successfully completed in less than an hour. As the smaller SPH particle size provides better resolution, therefore 2 mm SPH particle size was preferred over 3 mm.

Once compared with the Euler technique, material boundaries and interfaces in the SPH method are well defined and material separation is naturally handled [30]. Therefore, whether it's a quarter, half or full model, defining specific boundary conditions is not required in SPH technique.

Due to very fast reaction of detonation process (microsecond phenomena), a wrap-up time of 0.6 msec is assigned to the simulation process. The warhead was initiated by point detonation at one end of explosive fill (near end plate of cylinder). The detonation initiation point is depicted in red color diamond symbol in Fig 10.

To measure the blast parameters of expanding cylinder casing, 12 gauges (i.e., observation points) are designated on steel casing as shown in Fig 10. Gauges 1-4 are installed on near end of cylindrical casing along the Y-axis with a gap of 31 mm between them. Gauges 5-8 are installed along the length of cylindrical casing (Z-Axis) excluding both ends, with a gap of 90 mm between them. While, gauges 9-12 are installed on far end of cylindrical casing along the Y-axis with a gap of 31 mm between them. All these gauges are moving points and are capable to predict blast parameters even after fragmentation process.

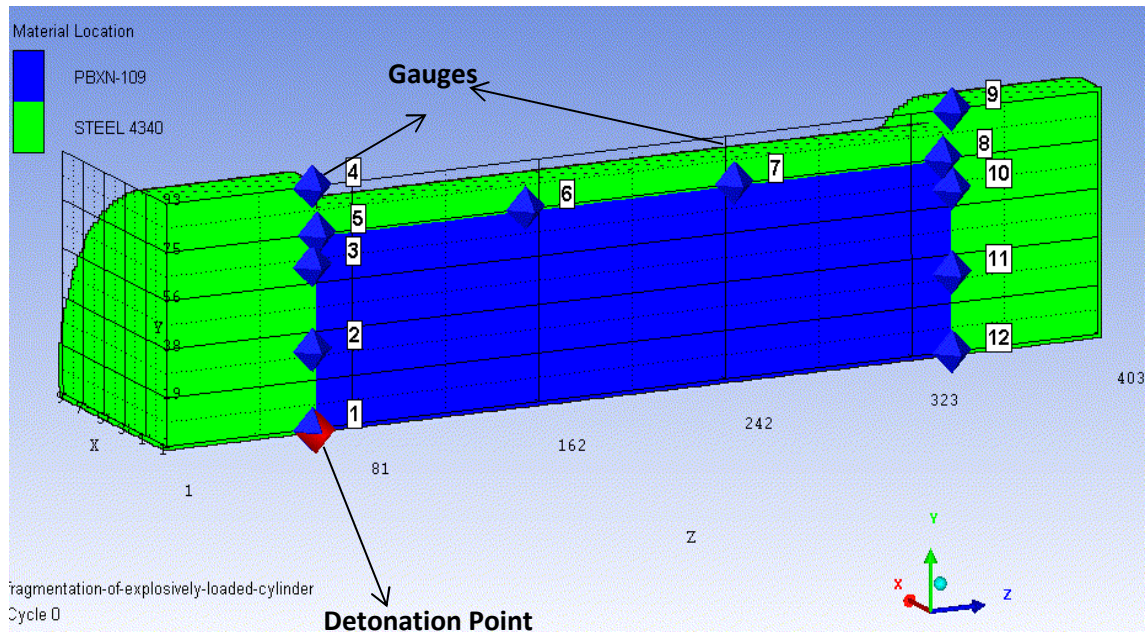


Figure 10: Location of Gauges and Detonation initiation Point on Simulated Warhead

3.7 Validation of Simulation Model

Prior to undertake comparative analysis of warhead casings, it is necessary to validate our simulation model with the experimental and simulation data available in literature. [26]. The model conditions used in Literature and in our simulation model are depicted in the table 6.

To achieve this objective, the selected thick-walled cylindrical warhead [26] was modelled in Autodyn with Steel Alloy AISI 4340 (equivalent material to EN24W steel) with PBXN-109 explosive. AISI 4340 Steel has been preferred over EN24 steel as it

already exists in Autodyn database and has been defined there using Johnson Cook parameters as shown in Figure 11.

Table 6: Comparison of Physical Parameters Simulation/Experimental Model

| Parameters | Simulation Results (this model) | Experimental Values [26] | Difference % |
|------------------------------|---|--------------------------|--------------|
| Warhead Casing Material | AISI 4340 Steel | EN24W Steel | - |
| Explosive Fill | PBXN-109 | PBXN-109 | - |
| Dimensions of Casing (mm) | Similar Dimensions (Inner Dia 150, Thickness 10 & Length 404) | | - |
| Total Mass of Warhead (Kg) | 47.225 | 47.21 | 0.032 |
| Explosive Fill Mass 'C' (Kg) | 8.038 | 8.01 | 0.35 |
| Mass of Casing 'M' (Kg) | 39.187 | 39.2 | 0.033 |
| Charge to Mass Ratio (C/M) | 0.205 | 0.2043 | 0.343 |

Rest all the modelling conditions were same except the casing material. Setup conditions like SPH particle size, detonation point, simulation wrap-up time etc. were kept same.

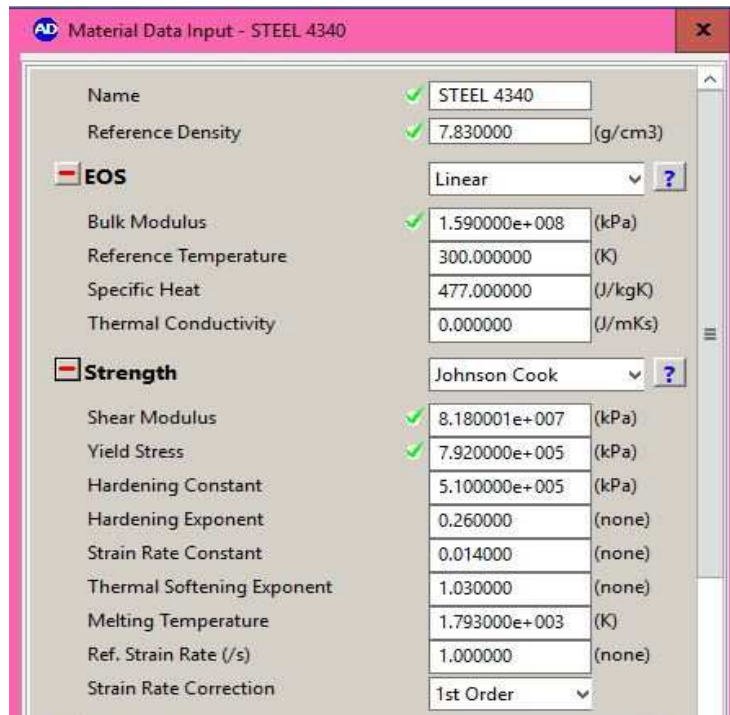


Figure 11: Johnson-Cook parameters for AISI 4340 Steel

The comparison between the simulation models and experimental results were based on parameters like Charge to Mass ratio (C/M), average fragments velocity, spatial distribution of fragments and the total number of fragments produced. The details of comparison are discussed in subsequent paragraphs.

3.7.1 Charge to Mass Ratio (C/M) After modelling in Autodyn, the mass of casing (AISI 4340) and explosive fill (PBXN-109) were noted. Fig 11 shows the total mass (of steel casing and explosive fill) vs time calculated in Autodyn software. As it is 1/4th model of the cylindrical warhead, therefore to calculate total mass of casing and explosives, we need to multiply it with 4. The total mass comes out to be 39.2 kg for casing and 8.01 kg for explosive fill, thus having C/M value of 0.2043. Whereas, the experimental values for mass of steel casing and explosive fill are 39.187 Kg and 8.038 respectively, having C/M as 0.205 [26]. Therefore, C/M values are almost same for both models.

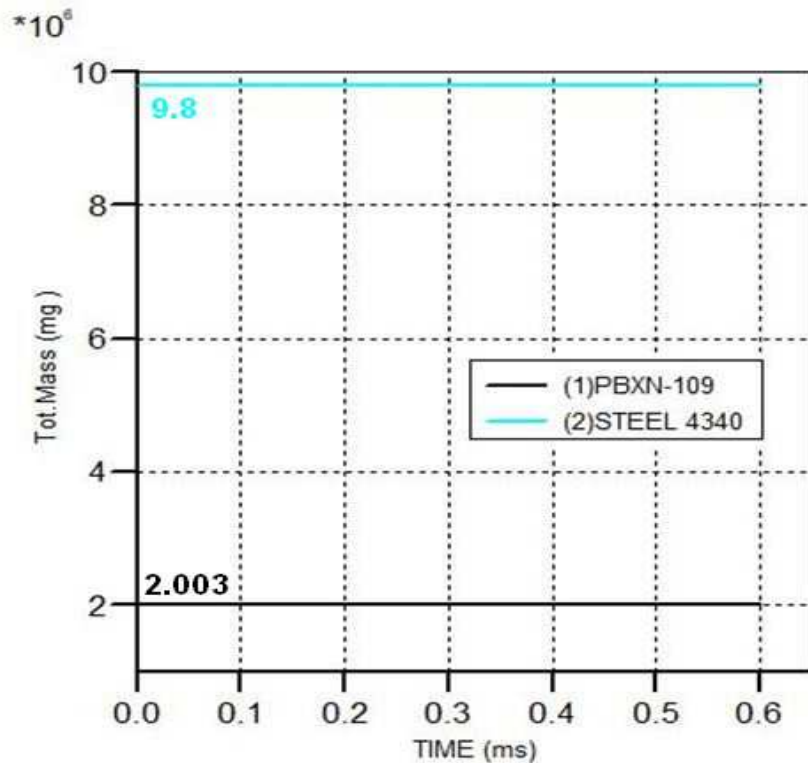


Figure 12: Total Mass Vs Time for Autodyn Simulation

3.7.2 Spatial Distribution of Fragments As the warhead has more wall thickness at both ends (i.e. 65 mm) of the cylinder as compared to central portion (i.e. 10 mm); therefore the maximum expansion is expected from the central portion of warhead. During the simulation with Autodyn, the fragmenting cylinder produced a ring type spatial distribution of fragments as shown in Fig 13 (left). Similar type of spatial distribution was observed in [26], when it was subjected to fragmentation process using GRIM software, as shown in Fig 13 (right). The spatial distribution of fragments depicted by Autodyn software is more clear and elaborative as compared to spatial distribution of fragments by GRIM software.

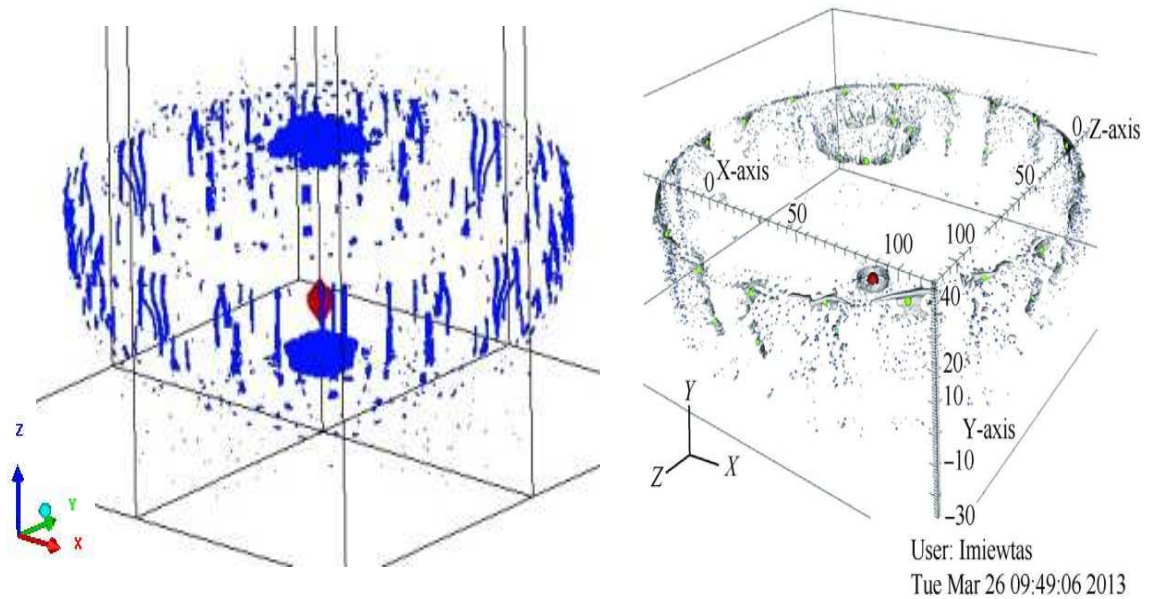


Figure 13: Spatial Distribution of Fragments in Autodyn (left) and in GRIM Software (Right)

3.7.3 Fragments Velocities

In Autodyn, the fragments velocities were predicted using installed gauges (1-12) on steel casing. Whereas, in the comparative experiment [26], fragments velocities were captured using velocity foils installed on straw board. The straw board was positioned at a distance of 3 meters from center of the

cylindrical warhead. Layout of the straw board used in experiment [26] is depicted in Fig 14. For a better comparison, the experimental values were translated against installed gauges and gauges 6 & 7 were found corresponding gauges for comparison, as depicted in Fig 14.

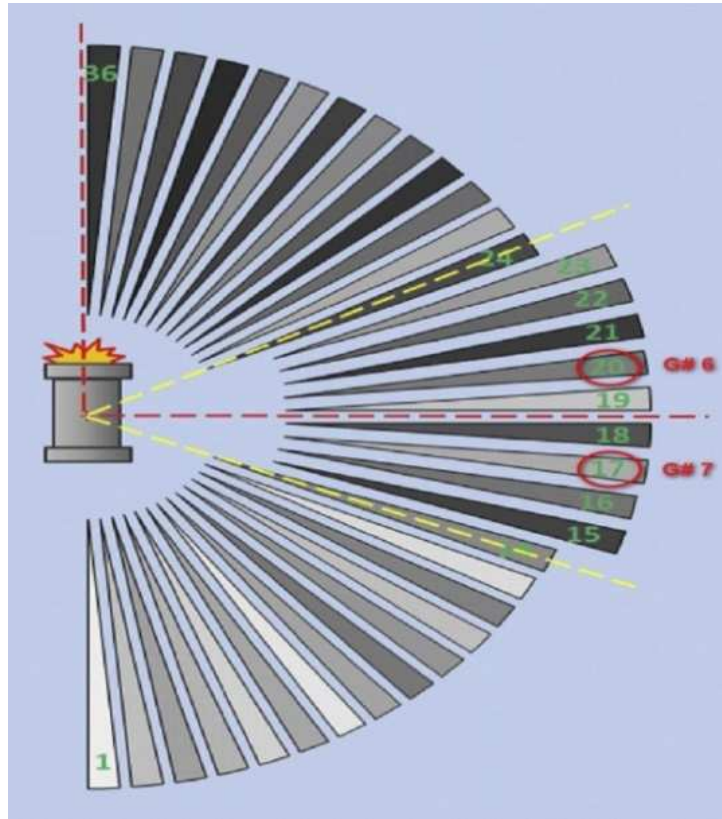


Figure 14: Translation of Angular Zones into Gauge Points

In Autodyn, the maximum fragments velocities were found close to center of warhead i.e., on gauge 6 and 7, as shown in Fig 15. The predicted fragments velocities were found in the range of 1455 to 1805 m/sec. The maximum fragment velocity was observed on gauge 7 i.e., 1615 m/sec. While, the experimental values of fragments velocities were found in the range of 1250 to 1800 m/sec [26].

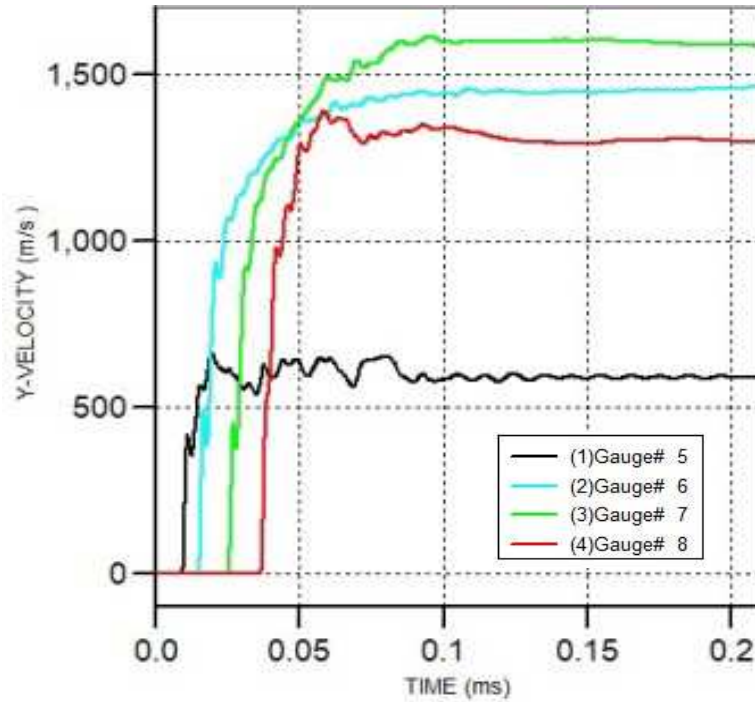


Figure 15: Y-Velocity Vs Time for Gauges 5-8

The comparative analysis of predicted fragments velocities by Autodyn (our Simulation model) and experimental results for gauges 6 and 7 is depicted in Table 7. There is a variation of 9-10% in fragment velocities. This much variation is always expected during such comparison, due to applying certain assumption in numerical analysis. Despite the small variations, the predicted values of fragment velocities (in Autodyn) are in good agreement to experimental values [26].

Table 7: Comparison of Initial Fragments Velocities

| Gauge Points | Simulation Results (this model) | Experimental Values [26] | Difference % |
|--------------|---------------------------------|--------------------------|--------------|
| Gauge#6 | 1455 | 1600 | 9 |
| Gauge#7 | 1615 | 1805 | 10.5 |

3.7.4 Total Fragments Produced

Upon completion of the simulation process using Autodyn, a total of 690 fragments (of varying sizes) were produced. Due to thick walls at ends of the cylinder (i.e. 65 mm thickness); fewer

fragments were produced at both ends. The spatial distribution of fragments produced during simulation process is shown in Fig 16.

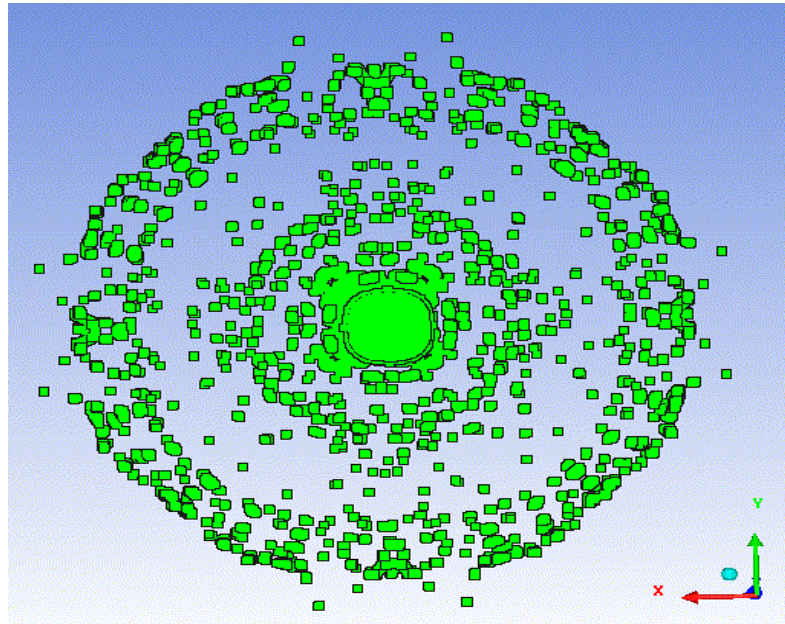


Figure 16: Side View of Spatial Distribution of Fragments

During the fragmentation process, both ends of the cylindrical warheads mostly remain intact due to comparatively thick walls. The central portion of the Fig 16 is depicting a large fragment, while the spatial distribution around it is formed by the small sized fragments produced by the central portion of warhead (having 10 mm thickness). Autodyn (SPH) provides detailed characteristics of each fragment i.e. mass, average velocity and dimension etc. Using mass of each individual fragment, mass distribution of fragments has been plotted as shown in Fig 17. The mass of maximum fragments produced are in the range of 1-5 gms.

Whereas, in the comparative experiment [26], 3 iterations were performed by detonating similar cylindrical warhead having same explosive charge. The number of fragments captured during these 3 iterations was 116, 111 and 122 respectively. Similarly, simulation of the same experiment using GRIM resulted in 128, 175 and 114 fragments experiment [26].

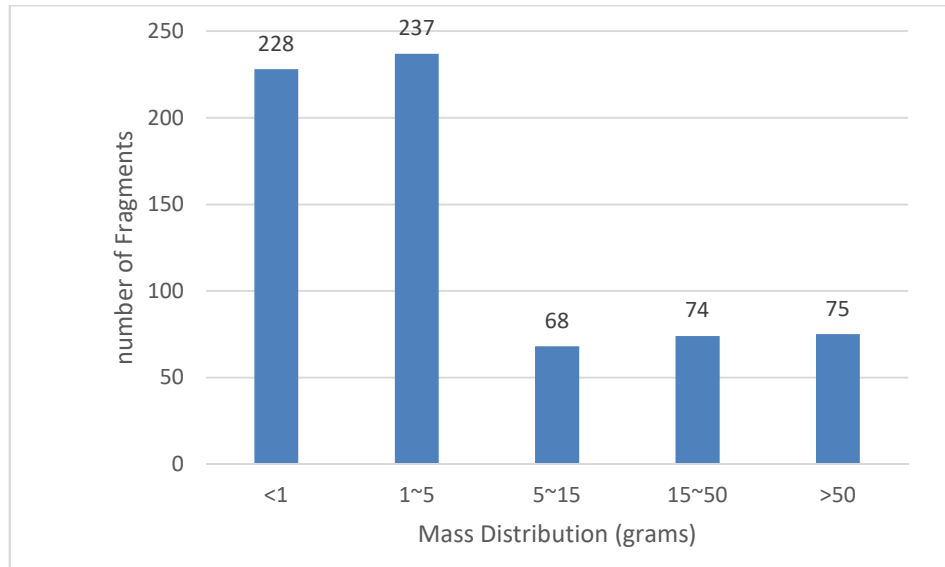


Figure 17: Mass distribution of fragments

The comparison of total number of fragments produced in our simulation model (Autodyn) and literature values are depicted in Table 8.

Table 8: Comparison of Fragments produced during experiment/simulation

| | Experimental Values* [26] | Simulation Values* (GRIM) | Simulation Results (this model) |
|--------------------------|----------------------------------|----------------------------------|--|
| Total Fragments Produced | 116 | 139 | 690 |

* Average Values

Large variation was observed w.r.t total number fragments produced, once our model i.e. Autodyn (SPH) results were compared with experimental / simulation results by GRIM [26]. Limited number of fragments was reported in experiment and simulation by GRIM. The main reason for this disparity is the limitation of fragments capturing mechanism used in experiment. As seen in Fig 13, the fragments capturing straw boards were installed on one side of warhead; therefore they are capturing fragments from a limited portion of warhead only. Moreover, all the fragments having mass ≤ 0.13 gm were excluded from experimental results [26]. Furthermore, GRIM software is based on Eulerian mesh, and identification of individual fragment is very difficult in this software

due to the presence of multi-mixed materials [26]. Therefore, a fragments identification algorithm is usually defined to identify individual fragments in GRIM software. That's may be the main reason that less number of fragments are identified in GRIM software.

On other hand, Autodyn predicts each single fragment produced during fragmentation process irrespective of its mass. Furthermore, capturing of fragments using straw boards is not considered very reliable approach and mostly high speed cameras are used to capture the blast/fragmentation phenomena.

3.7.5 Final Verdict on Validation of Our Simulation Model

The fragmentation process of thick-walled cylindrical warhead has been modelled in Autodyn (SPH solver) to determine blast parameters. The simulation results are compared with the experimental/simulation data (for similar warhead) available in literature [26]. The comparative analysis revealed that Autodyn provides the complete picture of fragmentation process. It also enables us to predict blast parameters (i.e., shock wave pressure, fragments velocity, number/size of fragments, fragments mass/spatial distribution etc.) which are otherwise difficult to measure in field experiments. The average fragments velocities predicted by Autodyn software were found in close approximation (variation of 9-10%) to the experimental values. The spatial distribution of fragments predicted by Autodyn and GRIM was almost identical. However, there was a variation with respect to total number of fragments produced during the simulation process and experimental results [26]. Less number of fragments was reported in experimental results as compared to Autodyn simulation. This is mainly due to the limitation of fragments capturing mechanism used during the experiment. Moreover, all fragments ≤ 0.13 gm were excluded from experimental results. Moreover, being Eulerian based software; GRIM has certain limitations for identification of individual fragments in multi-material mesh. On other hand, Autodyn predicts each single fragment produced during fragmentation process irrespective of its mass. That's the reason, that Autodyn has predicted much more fragments as compared to experimental results.

CHAPTER 4: RESULTS AND DISCUSSIONS

After validation of our simulation model (Autodyn with SPH Solver), comparative analysis of casing materials were undertaken. Numerous simulations were performed by varying casing materials to investigate the fragmentation behavior and to predict the blast parameters. In each simulation, similar thick-walled cylindrical warhead was used along with Compo B as an explosive fill. Setup conditions like SPH particle size, detonation point, simulation wrap-up time etc. were considered same as per para 3.6. The results of simulations conducted are discussed in subsequent paragraphs.

4.1 Expansion and rupture process of Warhead

Despite using the different casing material for each simulation, almost identical expansion and rupture behavior was observed. Upon initiation of detonation process, the expansion process started at near end of cylindrical warhead. Due to varying thickness of warhead casing at both ends (i.e., 65 mm) and along the length of cylinder (10 mm), the expansion of the cylinder mainly took place in radial direction. The expansion and rupture process of cylindrical warhead against time is shown in Fig 18a–d.

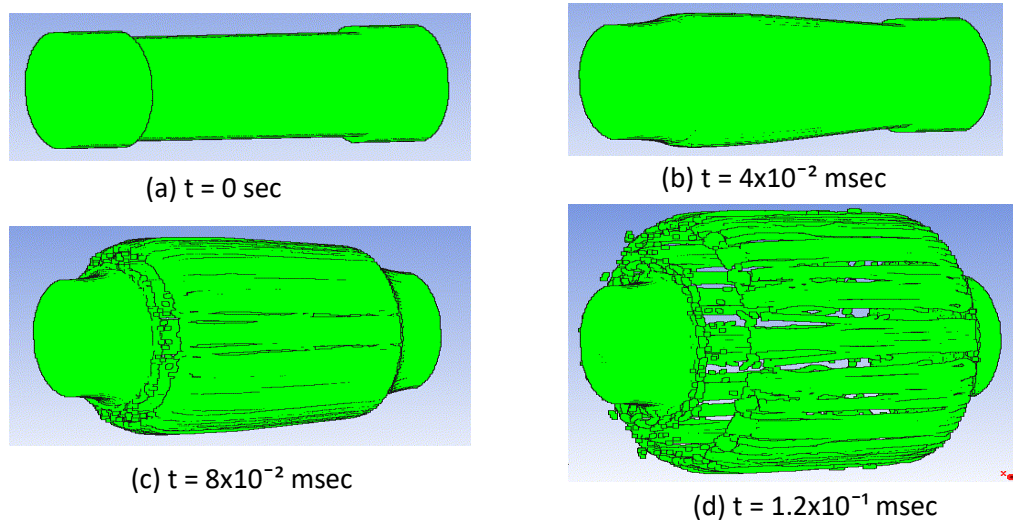


Figure 18: The expansion / rupture process of the cylindrical

Fig 18a presents the initial state, prior to initiation of warhead at $t=0$. Upon initiation of warhead, the cylindrical casing starts to expand radially from the near end, as shown in Fig 18b. As the detonate wave travels along the length of cylinder, the cylinder starts to expand radially and forms a cylindrical ring as shown in Fig 18c. While, there is very little deformation on both ends of warhead due to heavy walls. With the increasing expansion of cylindrical casing due to high pressure gaseous products of detonation process, fractures start to appear on circumference as shown clearly in Fig 18d.

Due to continuing expansion process of cylindrical casing , the fractures keep elongating until it rupture the casing into a number of high-velocity fragments [31]. Figure 16 shows the formation of fragments during the expansion process at time, $t= 0.4$ msec. Maximum fragments are produced at the circumference in radial direction, while minimum fragments are produced at both ends of the cylindrical warhead. Both near end and far end of cylinder mostly remain intact, due to heavy thickness of the casing at both ends and can be easily identified in Fig 19.

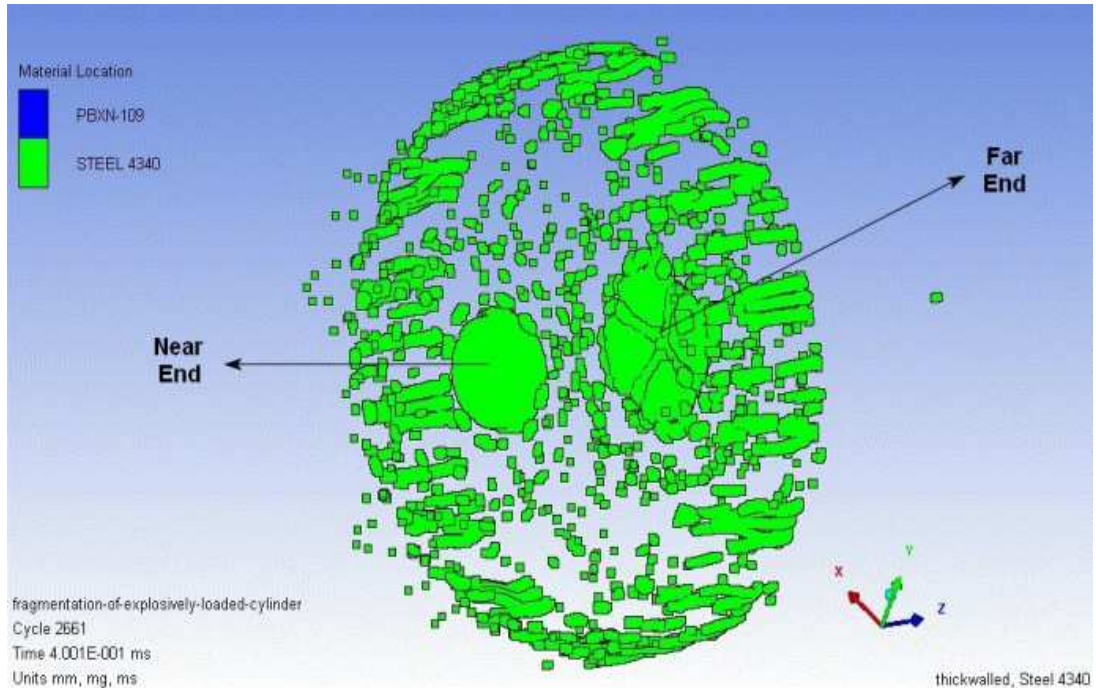


Figure 19: Formation of fragments from steel casing at time $t=0.4$ msec

4.2 Velocity of Fragments

It is one of the most important blast parameters of fragmented warheads as it defines the lethality of the warhead. Higher the fragments velocities, the more will be the range of warhead and fragments penetration into the target [10]. This initial fragment velocity is also useful to estimate the danger area. Since 2nd world war, lot of research work has been carried out in this field. To predict initial fragments velocities after the blast of fragmented warhead, classical Gurney's equations are widely used. However, Gurney's approach has some limitations that it doesn't cater the effects of the material properties of casing on blast parameters [10].

The selected warhead is now modelled in Autodyn (SPH Solver) using different casing materials already finalized in para 3.3. Each of the warheads was subjected to detonation to measure the blast parameters. As already mentioned, 12 moving gauges (observation points) were assigned on warhead casing to measure the blast parameters including initial fragments velocities. Using these gauges, the fragments velocities for each warhead were predicted.

Keeping in view the expansion and rupture process of warhead, fragments velocities of only gauges 5-8 will be predicted and considered for comparison. Fig 20 shows the gauges 5-8 installed on warhead casing to predict the fragment velocities.

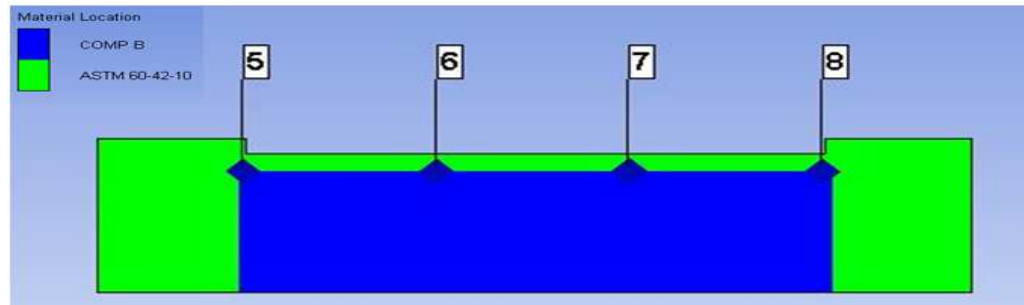


Figure 20: Gauges 5 - 8 installed on Warhead Casing

Details of numerical simulations carried out to predict initial fragments velocities of warheads (having different casing materials) are discussed in subsequent paragraphs.

4.2.1 A106 Grade C (Seamless Carbon Steel) The first casing material considered for blast/fragmentation analysis in Autodyn (SPH Solver) is A106 Grade C. As A106 Grade C is presently being used as casing material for PK-82 GP Bomb, therefore ballistic parameters of warhead (having A106 Grade C as casing material), will be considered as reference for comparison with other warheads (having different casing materials). The ASTM A106 specification is for seamless carbon steel pipes for high temperature service. As ASTM A106 is produced as a seamless product only therefore it doesn't have different types and it comes in three grades; A, B, C. As compared to grade A and B, grade C has maximum allowable carbon content; thus has higher mechanical properties.

Once thick-walled cylindrical warhead was modelled using A106 Grade C, the mass of casing and explosives comes out be 9.824 kg and 2.072 kg respectively. Using Gurney's equation for cylindrical warhead, the initial fragment velocity comes out to be 1212 m/sec [32]. The numerical simulation using Autodyn (SPH solver) predicted a maximum initial fragment velocity of 1905 m/sec. Fig 21 shows the fragments velocities vs time at gauges 5-8 for a warhead with casing material A106 grade C.

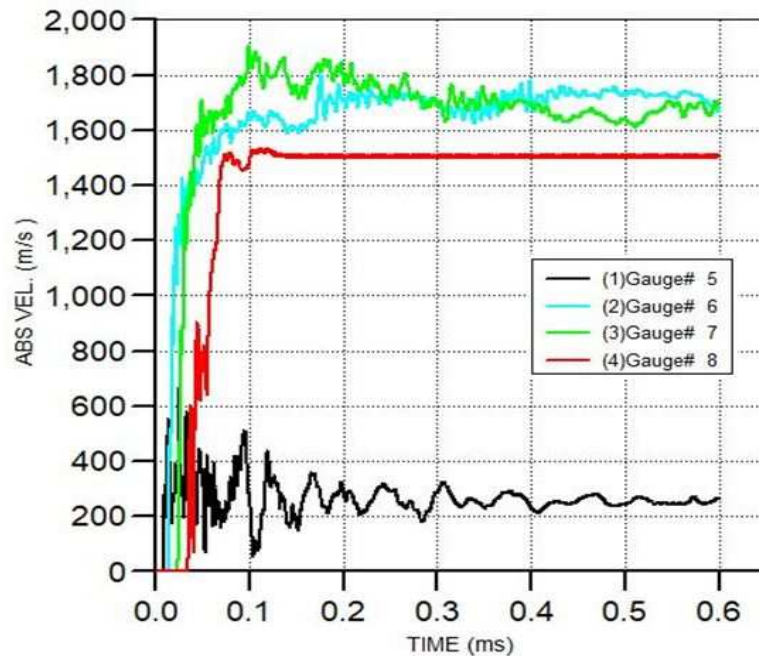


Figure 21: Fragments Velocities vs Time at Gauges 5-8

As the gauges 6 and 7 are located close to center of the warhead, therefore maximum fragments velocities are observed on these gauges. The maximum velocity at gauge 7 was observed at a time, $t=0.1$ m/sec. So, it can be assumed that 0.1 m/sec will be required for expansion/rupture process of warhead casing prior to formation of fragments. After the rupture of warhead casing, the blast gases will start to escape from these cracks. Therefore, the initial fragments formed will have maximum fragments velocities, once they exit from the influence of blast and same can be termed as initial fragments velocities.

To calculate the average velocity of fragments (in radial direction), only gauge 6 and 7 will be considered. Gauges 5 and 8 are located too close to ends of cylinder and will also have velocity component in Z-axis, that's why velocity readings of these gauges have been excluded. The maximum and minimum values of fragments velocities at gauges 6 and 7 are extracted from Autodyn and depicted in Fig 22.

| Plot | Minimum Y Value | | Maximum Y Value | |
|------|-----------------|-------------|-----------------|-------------|
| | X | Y | X | Y |
| 1 | 0.0000e+000 | 1.0000e-010 | 1.7641e-001 | 1.8028e+003 |
| 2 | 0.0000e+000 | 1.0000e-010 | 9.9942e-002 | 1.9055e+003 |

Figure 22: Max/Min Values of Fragments Velocities at Gauges 6 and 7

Fig 22 presenting the numerical values of fragments velocities (max/min) against the plot shown in Fig 21. Plot 1 and 2 in Fig 20 are representing the plots of gauges 6 and 7 respectively. The maximum values at gauges 6 and 7 comes out to be 1803 and 1905 m/sec respectively. Therefore, the average initial velocity of fragments for casing material A106 grade C comes out to be 1854 m/sec.

4.2.2 ASTM A27 Grade 65-35 (Cast Carbon Steel)

ASTM A27

is a carbon steel formulated for casting. It is widely used in automotive industry,

railways, construction machinery, mining equipment and engineering industries. In Carbon steels, only carbon is used as a principal alloying element. Other elements are present in very limited quantities, and are added for de-oxidation. Silicon and manganese typically range from 0.25 - 0.80% Si, While Mn ranges from 0.50 - 1.00% [33].

Once thick-walled cylindrical warhead was modelled using ASTM A27 Grade 65-35 (density 7.8 g/cm³), the mass of casing and explosives comes out be 9.762 kg and 2.072 kg respectively. Using Gurney's equation for cylindrical warhead, the initial fragment velocity comes out to be 1215 m/sec [32]. While, the numerical simulation using Autodyn (SPH solver) predicted a maximum initial fragment velocity of 1885 m/sec. Fig 23 shows the fragments velocities vs time at gauges 5-8 for a warhead with casing material ASTM A27 Grade 65-35.

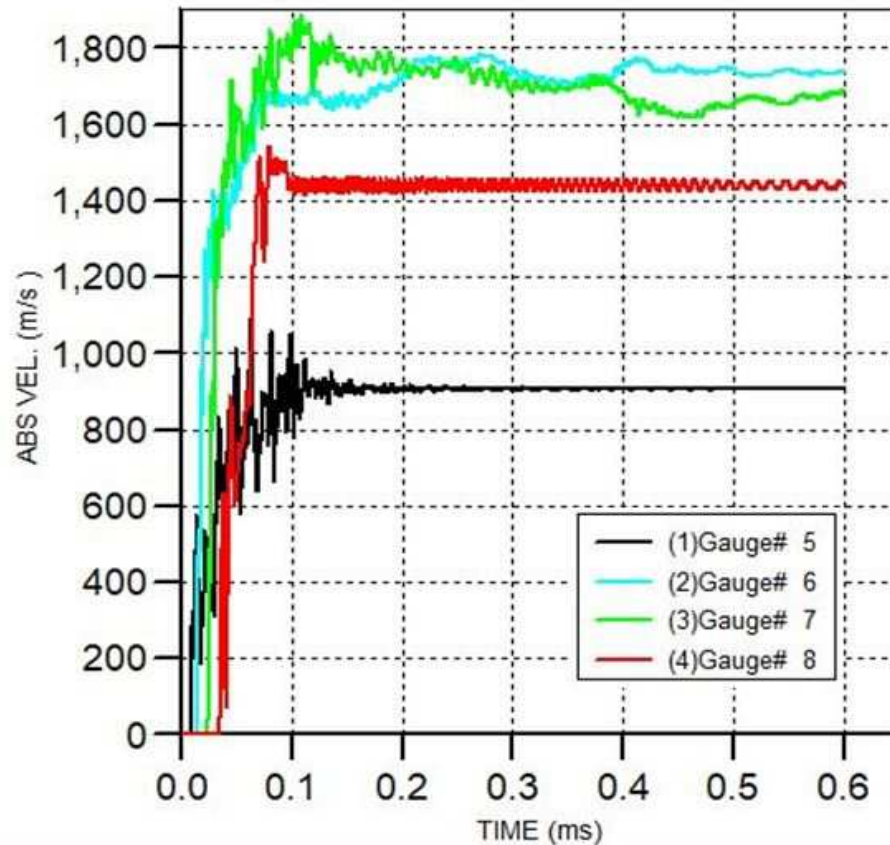
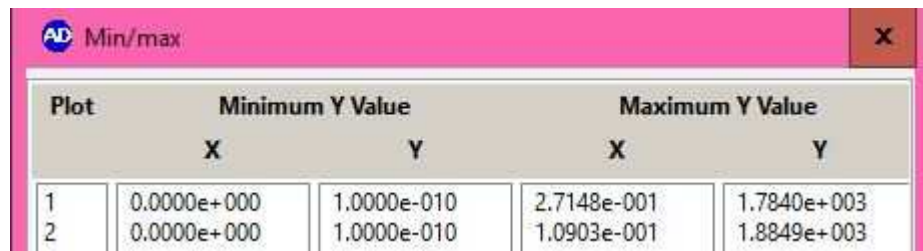


Figure 23: Fragments Velocities vs Time at Gauges 5-8 for ASTM A106 Gr C

To calculate average fragments velocities, maximum fragments velocity at gauges 6 and 7 were considered from Fig 24. The maximum values at gauges 6 and 7 were found 1784 and 1885 respectively. Therefore, the average initial fragments velocity for casing material ASTM 27 Grade 65-35 comes out to be 1835 m/sec.



| Plot | Minimum Y Value | | Maximum Y Value | |
|------|-----------------|-------------|-----------------|-------------|
| | X | Y | X | Y |
| 1 | 0.0000e+000 | 1.0000e-010 | 2.7148e-001 | 1.7840e+003 |
| 2 | 0.0000e+000 | 1.0000e-010 | 1.0903e-001 | 1.8849e+003 |

Figure 24: Max/Min Fragments Velocities at Gauges 6-8 for ASTM 27 Gr 65-35

4.2.3 ASTM A536 Grade 60-40-18 (Cast Ductile Iron)

ASTM 536 is an American standard specification that covers castings made of ductile iron, also known as nodular or spheroidal cast iron. Nodular or ductile cast iron is a more recent development. It is obtained by controlled and skillful introduction of molten magnesium into the iron, and small amounts of sulfur and phosphorus. Acquired in this way, it has a different microstructure in which the carbon is placed in the form of spheres in ferritic matrix. The change in microstructure results in a much stronger, elastic and durable iron. It has following compressive strengths like Abrasion resistance, ability to molding, fatigue and machinability. The main grades of ASTM A536 includes:-

- Grade 60-40-18
- Grade 60-42-10
- Grade 65-45-12
- Grade 70-50-05
- Grade 80-55-06
- Grade 80-60-03
- Grade 100-70-03

- Grade 120-90-02

ASTM A536 grade 60-40-18 is ductile cast iron in the annealed condition. Most ductile irons are designed for specific applications and requisite mechanical properties. ASTM A536 grade 60-40-18 has the lowest strength (minimum tensile strength of 414 MPa and yield strength of 276 MPa) and highest ductility (an elongation of 18%) compared to the other variants of ductile cast iron [33]. It is used to manufacture high pressure bearing parts for usage at high temperatures.

Once thick-walled cylindrical warhead was modelled using ASTM A536 grade 60-40-18 (density 7.1 g/cm³), the mass of casing and explosives comes out be 8.948 kg and 2.072 kg respectively. Using Gurney's equation for cylindrical warhead, the initial fragment velocity comes out to be 1264 m/sec [32]. While, the numerical simulation using Autodyn (SPH solver) predicted a maximum initial fragment velocity of 1973 m/sec. Fig 25 shows the fragments velocities vs time at gauges 5-8 for a warhead with casing material ASTM A536 grade 60-40-18.

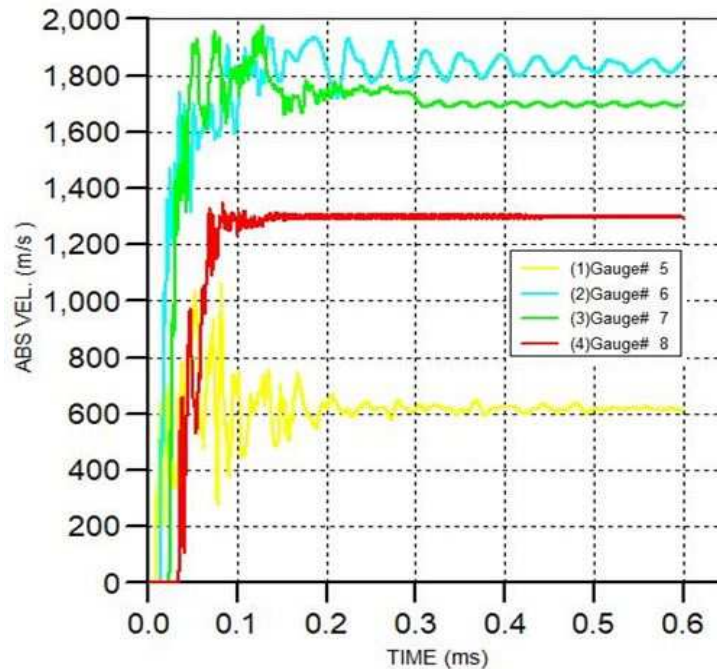


Figure 25: Fragments Velocities vs Time at Gauges 5-8 for warhead having casing material ASTM A536 Gr 60-40-18

To calculate average fragments velocities, maximum fragments velocity at gauges 6 and 7 were considered from Fig 26. The maximum values at gauges 6 and 7 were found 1935 and 1973 respectively. Thus, the average max initial fragments velocity for casing material comes out to be 1954 m/sec.

| Plot | Minimum Y Value | | Maximum Y Value | |
|------|-----------------|-------------|-----------------|-------------|
| | X | Y | X | Y |
| 1 | 0.0000e+000 | 1.0000e-010 | 1.8679e-001 | 1.9348e+003 |
| 2 | 0.0000e+000 | 1.0000e-010 | 1.2843e-001 | 1.9731e+003 |

Figure 26: Max/Min Values of Fragments Velocities at Gauges 6 & 7 for A536 Gr 60-40-18

4.2.4 ASTM Grade 40 (Grey Cast Iron) Grey cast iron is a type of cast iron, having grey appearance due to graphite flake structure that is formed during the cooling process. It has better machinability as compared to other types of cast irons and is widely used for production of industrial components. The graphite in gray cast iron has a flake-like structure which is largely responsible for the high machinability of this metal. The flake-like graphite structure gives rise to discontinuities in the metal matrix and subsequent reduced cutting forces. The main reason behind the popularity of grey cast iron components is their low cost. It has reasonable strength, ductility and impact resistance for most of the applications. Grade 40 cast iron is grey cast iron in the as-fabricated (no temper or treatment) condition.

Once thick-walled cylindrical warhead was modelled using ASTM Grade 40 (density 7.5 g/cm³), the mass of casing and explosives comes out be 9.386 kg and 2.072 kg respectively. Using Gurney's equation for cylindrical warhead, the initial fragment velocity comes out to be 1237 m/sec [32]. While, the numerical simulation using Autodyn (SPH solver) predicted a maximum initial fragment velocity of 2087 m/sec. Fig 27 shows the fragments velocities vs time at gauges 5-8 for a warhead with casing material ASTM Grade 40.

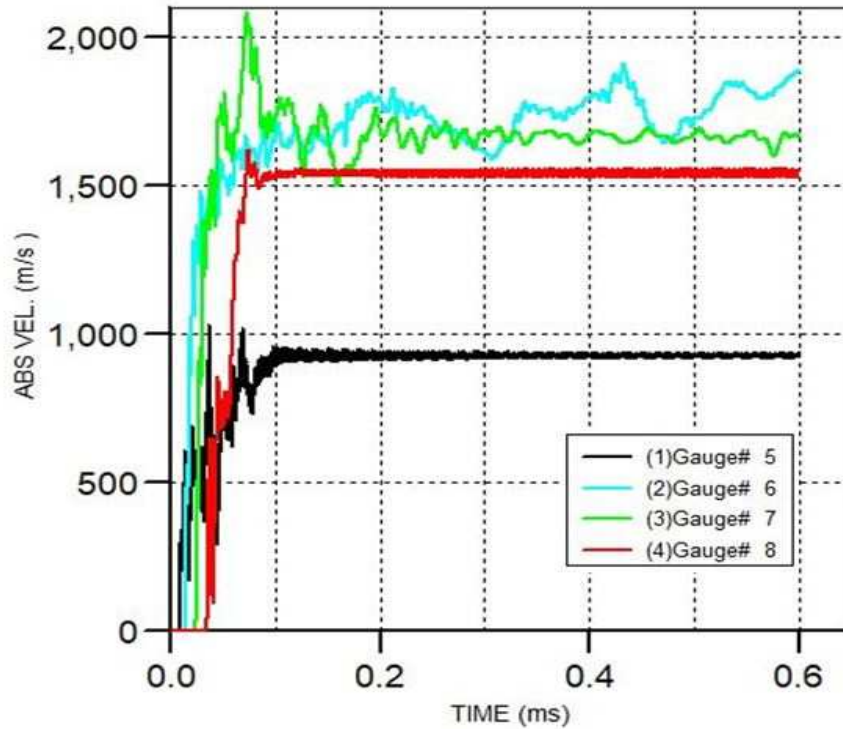


Figure 27: Fragments Velocities vs Time at Gauges 5-8 for casing material ASTM Grade 40

To calculate average fragments velocities, maximum fragments velocity at gauges 6 and 7 were considered from Fig 28. The maximum values at gauges 6 and 7 were found 1911 and 2087 respectively. Thus, the average max initial fragments velocity for casing material comes out to be 1999 m/sec.

| AD Min/max | | | | |
|------------|-----------------|-------------|-----------------|-------------|
| Plot | Minimum Y Value | | Maximum Y Value | |
| | X | Y | X | Y |
| 1 | 0.0000e+000 | 1.0000e-010 | 4.3337e-001 | 1.9106e+003 |
| 2 | 0.0000e+000 | 1.0000e-010 | 7.3114e-002 | 2.0867e+003 |

Figure 28: Max/Min Values of Fragments Velocities at Gauges 6 & 7 for ASTM Gr 40

4.2.5 ASTM A536 Grade 60-42-10 (Ductile Cast Iron)

ASTM A536

grade 60-42-10 is a special grade of cast ductile iron. It has average value of

tensile strength (min. 415 MPa), but the elongation% is high (min. 10%), which makes it strong and ductile alloy. ASTM A536 grade 60-42-10 is mostly used for special applications, such as pipes, fittings etc.

Once thick-walled cylindrical warhead was modelled using ASTM A536 grade 60-42-10 (density 7.5 g/cm³), the mass of casing and explosives comes out to be 9.011 kg and 2.072 kg respectively. Using Gurney's equation for cylindrical warhead, the initial fragment velocity comes out to be 1260 m/sec [32]. While, the numerical simulation using Autodyn (SPH solver) predicted a maximum initial fragment velocity of 2069 m/sec. Fig 29 shows the fragments velocities vs time at gauges 5-8 for a warhead with casing material ASTM A536 grade 60-42-10.

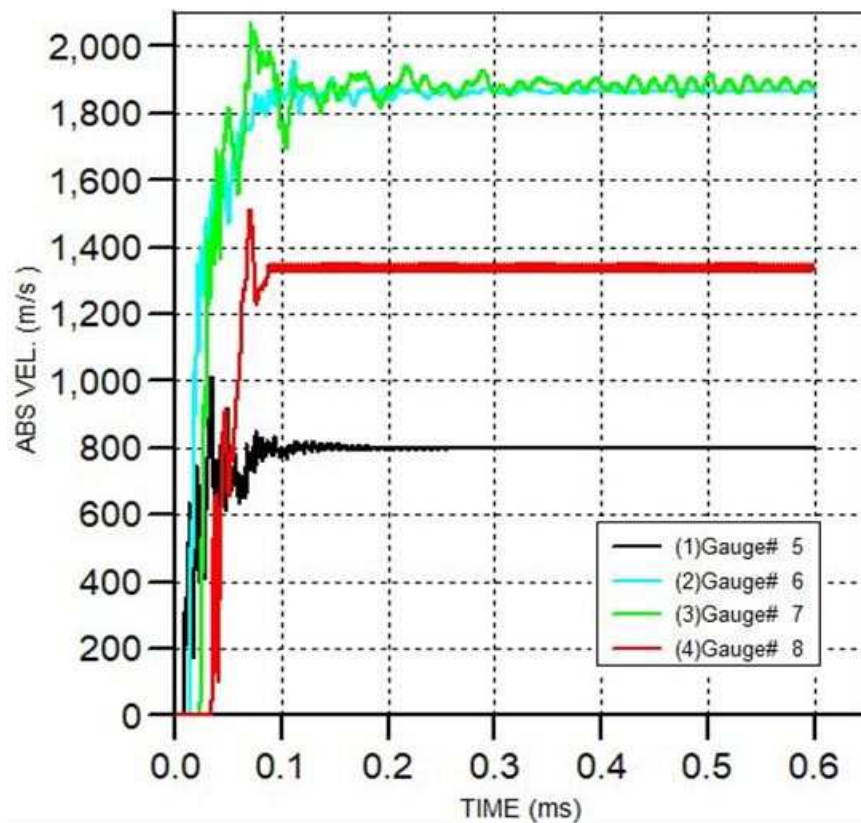


Figure 29: Fragments Velocities vs Time at Gauges 5-8 for warhead having casing material ASTM A536 Gr 60-42-10

To calculate average fragments velocities, maximum fragments velocity at gauges 6 and 7 were considered from Fig 30. The maximum values at gauges 6 and 7 were found 1954 and 2069 respectively. Thus, the average max initial fragments velocity for casing material comes out to be 2012 m/sec.

| Plot | Minimum Y Value | | Maximum Y Value | |
|------|-----------------|-------------|-----------------|-------------|
| | X | Y | X | Y |
| 1 | 0.0000e+000 | 1.0000e-010 | 1.1230e-001 | 1.9538e+003 |
| 2 | 0.0000e+000 | 1.0000e-010 | 7.1985e-002 | 2.0685e+003 |

Figure 30: Max/Min Values of Fragments Velocities at Gauges 6 & 7 for A536 Gr 60-42-10

4.2.6 Predicted Average Fragments Velocities The average fragments velocities of different warheads predicted by Autodyn SPH are displayed graphically in Figure 31. The reference material ASTM A106 Grade ‘C’ has an average fragments velocity of 1854 m/sec. The max average fragments velocity was predicted in warhead having casing material ASTM A536 Grade 60-42-10 i.e. 2012 m/sec.

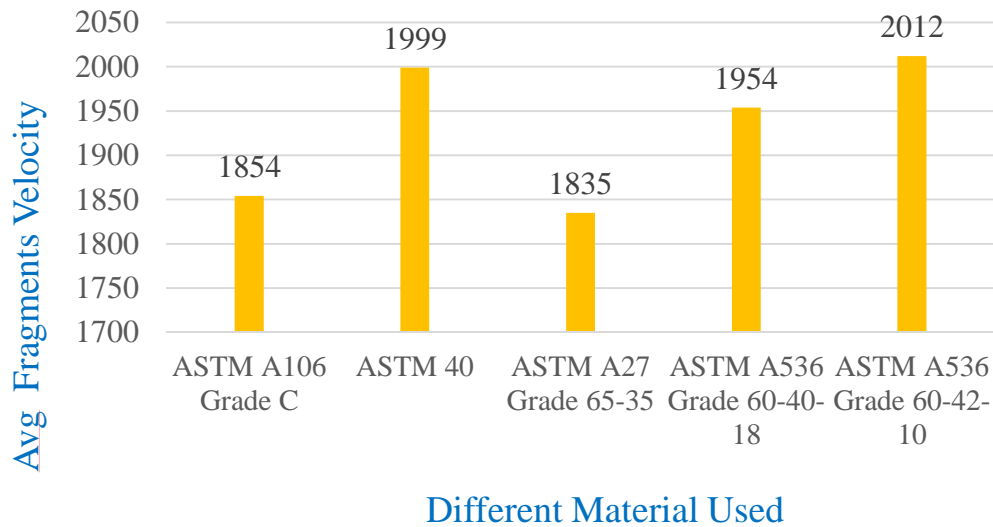


Figure 31: Predicted Average Fragments Velocity (Autodyn) for all Warheads

4.3 Fragmentation process

Fragmentation process of exploding warhead comprises of three main aspects i.e., total number of fragments produced, average size of fragments and spatial distribution of fragments. Higher the number of fragments more will be the probability of warhead to get damaged. Higher the mass of fragments more will be their lethality or ability to destroy the target. However, higher mass fragments will face more drag due to their higher mass and dimensions. Therefore, there should be a balance between the mass of fragments and the effective range of weapon. Due to this reason, the number of fragments produced and size of fragments will be area of focus during interpretation of fragmentation analysis.

4.3.1 Fragments Mass Distribution The casing material undergoes natural fragmentation after the blast. The propagation and size of fragment is random and dependent upon the shape of warhead. The dispersal pattern and size of the fragments is largely random. Despite using different casing materials, almost similar type of Mass distribution of fragments was observed for all warheads. Due to this reason, the average mass of fragments produced for all the warheads is almost same (refer table 10). Fig 32 shows the fragments mass distribution of warhead having casing material ASTM A106 Grade C (reference material).

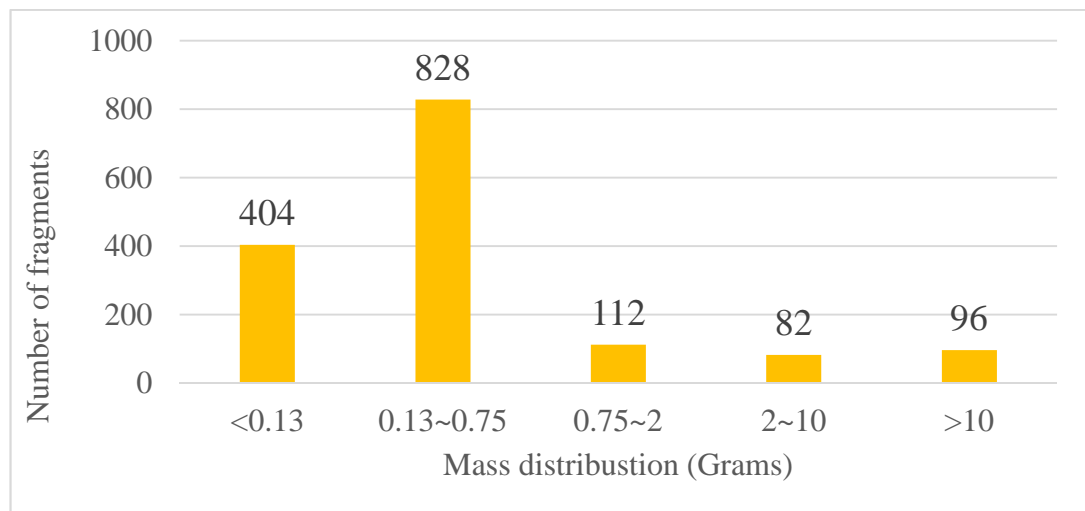


Figure 32: Fragments Mass Distribution for ASTM A106 Grade C

The fragments mass distribution mentioned in Table 10 is based on analysis of small fragments only and the 02 large sized fragments produced at both ends of cylinder (approx. mass 13-14 Kgs) have been excluded.

4.3.2 Total Number of Fragments Produced After completion of simulation process, fragmentation analysis reports were generated for all the warheads (with varying casing materials). As already mentioned Autodyn (SPH solver) caters each individual fragment as separate identity and provides detailed information of each fragment like mass, dimensions, average speed, momentum and kinetic energy etc. Table 9 presents the fragmentation behavior (i.e., total number of fragments produced and the average size of fragments) for each warhead.

Table 9: Summary of Fragmentation Analysis Report for Different Warheads

| Casing Materials | Total Fragments Produced | Average Size of Fragments (mg) |
|-----------------------------|---------------------------------|---------------------------------------|
| A106 Grade C | 1522 | 13.79 |
| ASTM 40 | 1536 | 13.79 |
| ASTM A27 Grade 65-35 | 1594 | 13.78 |
| ASTM A536 Grade 60-40-18 | 1558 | 13.79 |
| ASTM A536 Grade 60-42-10 | 1619 | 13.79 |

It is evident from the Table 9, that fragments mass distribution that average fragments mass is almost same for all the materials. Fig 33 represents the graphical representation of total number of fragments produced by each warhead in Autodyn. The reference material produced 1522 fragments while the

maximum fragments were produced by ASTM A536 Grade 60-42-10 i.e. 1619 fragments.

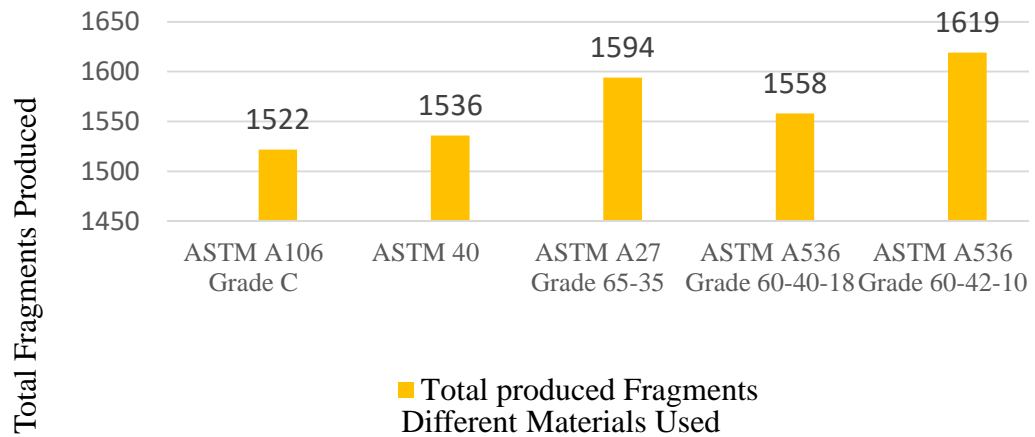


Figure 33: Predicted Total Number of Fragments (Autodyn) for all warhead casings

The extract from fragmentation analysis report of each casing material is depicted in Fig 34-38. Besides presenting the total number of fragments produced during the simulation process, these extracts are presenting summary of small particles. Furthermore, these extracts are depicting the properties of 03 individual fragments (sorted by mass, high to low) like mass, volume, kinetic energy, average speed etc.

Fragmentation Information Summary

Ident name: fragmentation-of-explosively-loaded-cylinder

Number of fragments: 1522

Unit system: (mm.mg.ms)

Time: 6.000E-01

Cycle: 3786

Total Mass: 4.758E+07

| Fragment Number | Elements in Fragment | Mass | Center-X | Center-Y | Center-Z | Origin-X | Origin-Y | Origin-Z | Volume | Characteristic Length | Kinetic Energy | Average Speed | X-Wise Momentum | Y-Wise Momentum | Z-Wise Momentum |
|-----------------|----------------------|-----------|----------|----------|----------|----------|----------|----------|-----------|-----------------------|----------------|---------------|-----------------|-----------------|-----------------|
| 1 | 226252 | 1.421E+07 | 0.00 | 0.00 | -112.59 | 0.00 | 0.00 | 32.46 | 1.811E+06 | 290.81 | 4.494E+11 | 251.50 | 0.000E+00 | 0.000E+00 | -3.573E+09 |
| 2 | 225984 | 1.419E+07 | 0.00 | 0.00 | 581.20 | 0.00 | 0.00 | 371.58 | 1.809E+06 | 290.19 | 1.003E+12 | 375.80 | 0.000E+00 | 0.000E+00 | 5.333E+09 |
| 3 | 7876 | 4.946E+05 | 731.06 | 731.09 | 262.73 | 56.30 | 56.31 | 200.64 | 6.316E+04 | 241.33 | 6.973E+11 | 1678.12 | 5.857E+08 | 5.857E+08 | 5.331E+07 |

Small Particle summary

| Total number | Total mass | Lowest Mass | Average Mass | Largest Mass | Total KE | Total Momentum |
|--------------|------------|-------------|--------------|--------------|-----------|----------------|
| 601153 | 8.288E+06 | 1.374E+01 | 1.379E+01 | 5.494E+01 | 7.968E+12 | 1.082E+10 |

Figure 34: Extract from Fragments Analysis Report of Casing Material A106

Fragmentation Information Summary

Ident name: fragmentation-of-explosively-loaded-cylinder

Number of fragments: 1594

Unit system: (mm.mg.ms)

Time: 6.001E-01

Cycle: 4055

Total Mass: 4.733E+07

| Fragment Number | Elements in Fragment | Mass | Center-X | Center-Y | Center-Z | Origin-X | Origin-Y | Origin-Z | Volume | Characteristic Length | Kinetic Energy | Average Speed | X-Wise Momentum | Y-Wise Momentum | Z-Wise Momentum |
|-----------------|----------------------|-----------|----------|----------|----------|----------|----------|----------|-----------|-----------------------|----------------|---------------|-----------------|-----------------|-----------------|
| 1 | 226160 | 1.411E+07 | 0.00 | 0.00 | 580.95 | 0.00 | 0.00 | 371.55 | 1.810E+06 | 299.43 | 9.961E+11 | 375.52 | 0.000E+00 | 0.000E+00 | 5.299E+09 |
| 2 | 218172 | 1.361E+07 | 0.00 | 0.00 | -115.40 | 0.00 | 0.00 | 31.44 | 1.746E+06 | 278.17 | 4.435E+11 | 255.25 | 0.000E+00 | 0.000E+00 | -3.475E+09 |
| 3 | 7125 | 4.446E+05 | 731.37 | 731.43 | 259.94 | 56.30 | 56.30 | 199.90 | 5.717E+04 | 229.35 | 6.269E+11 | 1677.94 | 5.265E+08 | 5.265E+08 | 4.626E+07 |

Small Particle summary

| Total number | Total mass | Lowest Mass | Average Mass | Largest Mass | Total KE | Total Momentum |
|--------------|------------|-------------|--------------|--------------|-----------|----------------|
| 601336 | 8.288E+06 | 1.374E+01 | 1.378E+01 | 5.494E+01 | 7.960E+12 | 1.084E+10 |

Figure 35: Extract from Fragments Analysis Report of Casing Material ASTM A27 Grade 65-35

Fragmentation Information Summary

Ident name: fragmentation-of-explosively-loaded-cylinder

Number of fragments: 1558

Unit system: (mm.mg.ms)

Time: 6.001E-01

Cycle: 4709

Total Mass: 4.408E+07

| Fragment Number | Elements in Fragment | Mass | Center-X | Center-Y | Center-Z | Origin-X | Origin-Y | Origin-Z | Volume | Characteristic Length | Kinetic Energy | Average Speed | X-Wise Momentum | Y-Wise Momentum | Z-Wise Momentum |
|-----------------|----------------------|-----------|----------|----------|----------|----------|----------|----------|-----------|-----------------------|----------------|---------------|-----------------|-----------------|-----------------|
| 1 | 225452 | 1.290E+07 | 0.00 | 0.00 | -126.74 | 0.00 | 0.00 | 32.38 | 1.804E+06 | 308.78 | 5.465E+11 | 291.09 | 0.000E+00 | 0.000E+00 | -3.754E+09 |
| 2 | 217096 | 1.242E+07 | 0.00 | 0.00 | 592.79 | 0.00 | 0.00 | 372.69 | 1.737E+06 | 286.72 | 9.599E+11 | 393.12 | 0.000E+00 | 0.000E+00 | 4.882E+09 |
| 3 | 7071 | 4.045E+05 | 1081.12 | 75.10 | 263.57 | 78.56 | 13.03 | 203.45 | 5.671E+04 | 254.36 | 6.307E+11 | 1765.04 | 7.117E+08 | 3.730E+07 | 4.233E+07 |

Small Particle summary

| Total number | Total mass | Lowest Mass | Average Mass | Largest Mass | Total KE | Total Momentum |
|--------------|------------|-------------|--------------|--------------|-----------|----------------|
| 601112 | 8.288E+06 | 1.374E+01 | 1.379E+01 | 5.494E+01 | 8.352E+12 | 1.112E+10 |

Figure 36: Extract from Fragments Analysis Report of Casing Material A536 Grade 60-40-18

Fragmentation Information Summary

Ident name: fragmentation-of-explosively-loaded-cylinder

Number of fragments: 1536

Unit system: (mm.mg.ms)

Time: 6.000E-01

Cycle: 5812

Total Mass: 4.583E+07

| Fragment Number | Elements in Fragment | Mass | Center-X | Center-Y | Center-Z | Origin-X | Origin-Y | Origin-Z | Volume | Characteristic Length | Kinetic Energy | Average Speed | X-Wise Momentum | Y-Wise Momentum | Z-Wise Momentum |
|-----------------|----------------------|-----------|----------|----------|----------|----------|----------|----------|-----------|-----------------------|----------------|---------------|-----------------|-----------------|-----------------|
| 1 | 224068 | 1.344E+07 | 0.00 | 0.00 | 590.49 | 0.00 | 0.00 | 371.79 | 1.793E+06 | 302.90 | 1.085E+12 | 401.65 | 0.000E+00 | 0.000E+00 | 5.400E+09 |
| 2 | 221384 | 1.328E+07 | 0.00 | 0.00 | -117.06 | 0.00 | 0.00 | 31.88 | 1.771E+06 | 277.93 | 4.277E+11 | 253.78 | 0.000E+00 | 0.000E+00 | -3.370E+09 |
| 3 | 9064 | 5.438E+05 | 1057.30 | 0.00 | 248.04 | 70.24 | 0.00 | 102.14 | 7.270E+04 | 303.41 | 8.007E+11 | 1722.61 | 9.351E+08 | 0.000E+00 | 5.621E+07 |

Small Particle summary

| Total number | Total mass | Lowest Mass | Average Mass | Largest Mass | Total KE | Total Momentum |
|--------------|------------|-------------|--------------|--------------|-----------|----------------|
| 600997 | 8.287E+06 | 1.374E+01 | 1.379E+01 | 5.494E+01 | 8.099E+12 | 1.093E+10 |

Figure 37: Extract from Fragments Analysis Report of Casing Material ASTM Grade 40

Fragmentation Information Summary

Ident name: fragmentation-of-explosively-loaded-cylinder

Number of fragments: 1619

Unit system: (mm.mg.ms)

Time: 6.001E-01

Cycle: 3748

Total Mass: 4.433E+07

| Fragment Number | Elements in Fragment | Mass | Center-X | Center-Y | Center-Z | Origin-X | Origin-Y | Origin-Z | Volume | Characteristic Length | Kinetic Energy | Average Speed | X-Wise Momentum | Y-Wise Momentum | Z-Wise Momentum |
|-----------------|----------------------|-----------|----------|----------|----------|----------|----------|----------|-----------|-----------------------|----------------|---------------|-----------------|-----------------|-----------------|
| 1 | 223740 | 1.289E+07 | 0.00 | 0.00 | -121.31 | 0.00 | 0.00 | 32.17 | 1.790E+06 | 292.10 | 4.542E+11 | 265.44 | 0.000E+00 | 0.000E+00 | -3.421E+09 |
| 2 | 219452 | 1.264E+07 | 0.00 | 0.00 | 591.92 | 0.00 | 0.00 | 372.35 | 1.757E+06 | 290.84 | 9.793E+11 | 393.33 | 0.000E+00 | 0.000E+00 | 4.972E+09 |
| 3 | 7954 | 4.177E+05 | 1075.49 | 0.00 | 259.07 | 70.54 | 0.00 | 122.17 | 5.048E+04 | 354.04 | 6.464E+11 | 1759.17 | 7.208E+08 | 0.000E+00 | 4.248E+07 |

Small Particle summary

| Total number | Total mass | Lowest Mass | Average Mass | Largest Mass | Total KE | Total Momentum |
|--------------|------------|-------------|--------------|--------------|-----------|----------------|
| 600856 | 8.288E+06 | 1.374E+01 | 1.379E+01 | 5.494E+01 | 8.281E+12 | 1.106E+10 |

Figure 38: Extract from Fragments Analysis Report of Casing Material A536 Gr 60-42-

4.4 Comparative Analysis of Results

After predicting the blast parameters of thick-walled cylinder warhead (using Autodyn (SPH Solver), a comparative analysis has been carried out between warheads (of different casing materials). The main parameters considered for comparison are average fragments velocities and total number of fragments produced during the fragmentation process. All warheads considered for comparison have similar geometry/dimensions and same explosive fill inside but different casing material. The comparative analysis of both predicted parameters during various simulations is depicted in Table 11:-

Table 10: Comparative Analysis of Total Number of Fragments Produced

| Casing Materials | Total Fragments Produced | % Increase | Average Fragments Velocity (m/sec) | % Variation |
|---|---------------------------------|--------------------|---|--------------------|
| ASTM A106 Grade C (Cast Carbon Steel) | 1522 | Reference Material | 1854 | Reference Material |
| ASTM 40 (Grey Cast Iron) | 1536 | 0.92 | 1999 | 7.82 |
| ASTM A27 Grade 65-35 (Cast Carbon Steel) | 1594 | 4.73 | 1835 | -0.01 |
| ASTM A536 Grade 60-40-18 (Cast Ductile Iron) | 1558 | 2.37 | 1954 | 5.39 |
| ASTM A536 Grade 60-42-10 (Cast Ductile Iron) | 1619 | 6.37 | 2012 | 8.52 |

All the selected materials produces slightly more fragments as compared to reference material i.e., A106 Grade C. The maximum number of fragments produced by a warhead having casing material ASTM A536 Grade 60-42-10, which are 1619 fragments (6.4% more than reference casing material).

Similarly, all the selected materials (except ASTM A27 Cast Carbon Steel) gave higher average fragments velocities as compared to reference material. The maximum

average fragments velocities was observed in warhead having casing material ASTM A536 Grade 60-42-10, which is 2012 m/sec (8.5% more than reference casing material).

Warheads having cast ductile iron casing material showed excellent fragmentation characteristics during the numerical simulation. Two different alloys of Cast Ductile Iron were considered in comparative analysis (i.e., ASTM A536 60-40-18 and ASTM 60-42-10), both materials showed improvement in terms of initial fragments velocities and number of fragments produced, once compared with reference material i.e., ASTM A106 Grade C.

4.5 Comparison of Physical Properties

As cased munitions are subjected to long term storage, extreme environments conditions and loads during launch and drop sequence, therefore these munitions must have extra ordinary physical properties like strength, impact and corrosion resistance etc.

Keeping in view the comparative analysis of blast parameters i.e., total number of fragments produced and initial fragments velocities, cast ductile iron was found more suitable as a casing material for fragmented warheads due to its better fragmentation characteristics. However, prior to consider it as a replacement to existing materials, it is better to undertake comparison of both materials on basis of different physical properties. Details of the comparison are as follows:-

4.5.1 Composition/ Structure Ductile iron has higher carbon content (3.0%-3.9%) than cast steel (0.08%-0.60%). Due to limited carbon content in cast steel, carbon does not form free graphite, thus resulting in a laminate type structure. While in Ductile Iron, graphite flakes are modified by a skill full treatment process to form tiny spheres or nodules. This modified microstructure of cast ductile Iron provides it the physical properties like steel [34].

4.5.2 Strength Cast ductile Iron alloys are much stronger as compared to cast iron alloys. Both cast steel and ductile iron has almost similar values of tensile strength but yield strength of ductile iron has higher value than cast steel.

The comparison of strength between cast ductile iron alloy and cast carbon steel alloy is presented in table 10 [34]. It is evident from table 10 that as the strength of cast ductile iron alloy is increases its ductility decreases.

Table 11: Comparison of Strength between Cast Ductile Iron vs Cast Steel

| ASTM A536 Cast Ductile Iron | | | | ASTM A27 Cast Carbon Steel | | | |
|-----------------------------|---------------------------------|----------------------|----------------|----------------------------|---------------------------------|----------------------|----------------|
| Grades | Ultimate Tensile Strength (ksi) | Yield Strength (ksi) | Elongation (%) | Grades | Ultimate Tensile Strength (ksi) | Yield Strength (ksi) | Elongation (%) |
| 60-42-18 | 60 | 40 | 18 | 60-30 | 60 | 30 | 22 |
| 65-45-12 | 65 | 45 | 12 | 65-35 | 65 | 35 | 24 |
| 80-55-6 | 80 | 55 | 6 | 70-36 | 70 | 36 | 22 |

4.5.3 Shock Absorption Cast ductile iron has better shock absorption as compared to cast carbon steel. Shock absorption is dependent on degree of ferritization in microstructure. The average damping capacity of a cast ductile iron is 6.6 times greater than SAE 1018 steel [34]. Due to this reason, ductile iron is considered best for warheads that impact the targets.

4.5.4 Weldability Cast carbon steel has better weldability as compared to cast ductile iron. However, proper welding can be achieved in ductile iron by following specialized welding procedures [34].

4.5.5 Abrasion Resistance Cast ductile iron has superior abrasion resistance and it is even comparable to some of the best grades of steel. Due to this reason, cast ductile iron is normally used in friction wear components e.g. engine crankshafts. The presence of higher percentage of graphite is the main reason behind its better abrasion resistance which acts as a lubricant [34].

4.5.6 Corrosion Resistance Cast ductile iron alloys have superior corrosion/oxidation resistance as compared to cast carbon steel and even better

than highly alloyed steels in certain environment conditions. Oxide penetration may severely affect the performance and strength of an alloy [34].

4.6 Cost Effectiveness

Cast ductile iron alloys not only offers high performance and versatility but also a cost effective substitute for cast carbon steels. During solidification process of commercial cast metals, decrease in volume occurs, which causes shrinkage (internal/external) of structure. Therefore, addition metal is poured from a reservoir to avoid these defects. However, in case of ductile iron castings, graphite is formed during the solidification process, which causes internal expansion of ductile iron. Due to this reason, ductile iron alloys doesn't require additional feed metal. This provides a substantial cost saving with respect to limited requirement of material and power consumption. Furthermore, it is less brittle than most types of iron and can be used in the as-cast condition without additional heat treatments. Table 12 presents the cost comparison of existing casing material i.e., ASTM A106 Grade C and Cast Ductile Iron ASTM A536 Grade 60-42-10.

Table 12: Cost Comparison between Cast Ductile Iron Vs Cast Carbon steel

| Material Grade | Price (USD/KG) |
|---|-----------------------|
| Cast Ductile Iron ASTM A536 Grade 60-42-10 | 1.31 |
| Cast Carbon Steel ASTM A106 Grade C | 2.40 |

(Source:<http://www.iron-foundry.com/ductile-iron-properties-advantages-costs-capability.html>)

4.7 Improved Lethality Warhead (ILW) program

The Improved Lethality Warhead (ILW) program is an effort to increase lethality of GP Bombs to enhance the area attack capability of USAF (United States Air Force) fighter aircraft. The project was started in year 2015 and was aimed to improve fragmentation characteristics of existing GP bombs in future scenarios. After

considering different options, improvement in lethality was recommended by replacing the existing steel casing with an alternative material, which produces much better fragmentation than warheads with conventional steel casing.

In FY 2016, USAF started manufacturing of prototype BLU-134/B Improved Lethality Warhead (ILW) using cast ductile iron as a casing material for the bomb body. Cast ductile iron was finalized as casing material on basis of its excellent fragmentation characteristics observed during the testing phase. Beside better fragmentation, cast ductile iron has excellent physical properties (like tensile strength, impact resistance, shock absorption, weldability, corrosion resistance and abrasion resistance etc.), and it can handle extreme environments conditions (like vibrations, maneuvering loads, extreme temperatures, etc.) during flight and drop sequence from fighter aircraft. Subsequent to its aerial trials and arena testing results, same will be subjected to serial production.

Conclusion

The comparative analysis of blast parameters of various fragmented warheads (with different casing material) has been demonstrated using Autodyn (SPH solver). A thick-walled cylindrical warhead was chosen from available literature and subjected to fragmentation analysis using Autodyn. Blast parameters like shock wave pressure, initial fragments velocities, number/size of fragments produced, mass/spatial distribution of fragments etc. were predicted by installing gauges (i.e., observation points) on warhead casing. The simulation results were validated by comparing it with the experimental/simulation data available in literature. Subsequently, thick-walled cylindrical warhead was modelled in Autodyn using different casing materials and a set of simulations were performed to evaluate the performance of each casing material.

Comparative analysis revealed that cast ductile iron casing's provides better fragmentation characteristics as compared to other iron alloys. Warhead with casing material ASTM A536 Grade 60-42-10 Cast Ductile Iron produced maximum number of fragments and maximum fragments velocities.

In addition, cast ductile iron has high performance features like improved castability, increased strength, superior shock absorption and excellent corrosion/abrasion resistance. Furthermore, cast ductile iron has low cost as compared to cast steel as it requires limited material resources and less energy resources (i.e., heat treatment).

The comparative analysis result also got validated by the findings of Improved Lethality Warhead (ILW) program, initiated by USA Department of Defense (DoD), which also recommends used of cast ductile iron as a casing material for its GP Bombs.

It has also been concluded that Autodyn (SPH solver) is a better technique to simulate fragmentation process of cased munitions. It not only provide better understanding of fragmentation process but can also assist to determine blast parameters, which are otherwise difficult to measure in field experiments. Furthermore, it analyzes each and every fragment produced during the fragmentation process and provides

detailed information of each fragment like mass, dimensions, average speed, momentum and kinetic energy etc.

Last but not the least, the improvement in performance of PK-82 GP Bomb will be benefitting for Research and Development (R&D) setup of Pakistan Ordnance Factories (POF), Wah Cantt and PAF Munitions Filling Factory, Malir Cantt, Karachi.

Recommendations

The above mentioned fragmentation analysis technique is specifically applicable to cylindrical warheads but can also be generalized to any type of cased munitions. To get more accuracy and reliability in prediction of blast parameters, it is suggested that MK-82GP Bombs may be modelled in Autodyn as per actual/scale down dimensions.

In this research, due to paucity of time, only 02 grades of cast ductile iron were considered for fragmentation analysis. Remaining grades may also be considered in future work to establish a better casing material for cased munitions.

In addition, concept employed in pre-frag bombs i.e., marking a pre-scored seams along length/ width on inner side of bomb body, can also be modelled in Autodyn, to further improve the fragmentation characteristics.

References

- [1] N. A. S. C. Commander, "Joint Munitions Effectiveness Manual," 1974.
- [2] J. Pearson, "A fragmentation model for cylindrical warheads," NAVAL WEAPONS CENTER CHINA LAKE CA1990.
- [3] B. Zecevic, J. Terzic, A. Catovic, and S. Serdarevic-Kadic, "Influencing parameters on HE projectiles with natural fragmentation," in *International Conference on New Trends in Research of Energetic Materials*, 2006, pp. 780-795.
- [4] W. Walters, "A brief history of shaped charges," ARMY RESEARCH LAB ABERDEEN PROVING GROUND MD WEAPONS AND MATERIALS RESEARCH ...2008.
- [5] H. Y. Grisaro and A. N. J. I. J. o. I. E. Dancygier, "Characteristics of combined blast and fragments loading," vol. 116, pp. 51-64, 2018.
- [6] H. Grisaro and A. N. J. I. J. o. I. E. Dancygier, "Numerical study of velocity distribution of fragments caused by explosion of a cylindrical cased charge," vol. 86, pp. 1-12, 2015.
- [7] Y. Li, Y.-h. Li, and Y.-q. J. I. j. o. i. e. Wen, "Radial distribution of fragment velocity of asymmetrically initiated warhead," vol. 99, pp. 39-47, 2017.
- [8] M. D. I. Blackwelder, *The long road to Desert Storm and beyond: the development of precision guided bombs*. Pickle Partners Publishing, 2015.
- [9] R. W. Gurney, "The initial velocities of fragments from bombs, shell and grenades," Army Ballistic Research Lab Aberdeen Proving Ground Md1943.
- [10] G. Tanapornraweekit, W. J. W. A. o. S. Kulsirikasem, Engineering, and Technology, "Effects of material properties of warhead casing on natural fragmentation performance of high explosive (HE) warhead," vol. 59, pp. 1275-1280, 2011.
- [11] U. J. A. B. R. L. Fano, Report BRL, "Methods for Computing Data on the Terminal Ballistics of Bombs–II Estimation of the Air Blast," vol. 524, 1944.
- [12] E. Fisher, "The effect of the steel case on the air blast from high explosives," NAVAL ORDNANCE LAB WHITE OAK MD1953.

- [13] N. F. J. P. o. t. R. S. o. L. S. A. M. Mott and p. sciences, "Fragmentation of shell cases," vol. 189, no. 1018, pp. 300-308, 1947.
- [14] L. E. Mott N., "A Theory of Fragmentation. In: Fragmentation of Rings and Shells. Shock Wave and High Pressure Phenomena," 2006. Springer, Berlin, Heidelberg
- [15] D. Grady and M. Hightower, "Natural fragmentation of exploding cylinders," Sandia National Labs., Albuquerque, NM (USA)1990.
- [16] W. Arnold and E. J. I. j. o. i. e. Rottenkolber, "Fragment mass distribution of metal cased explosive charges," vol. 35, no. 12, pp. 1393-1398, 2008.
- [17] M. Hutchinson, "The escape of blast from fragmenting munitions casings," *International Journal of Impact Engineering*, no. 36, pp. 185-192, 2009.
- [18] M. D. Hutchinson, "Replacing the Equations of Fano and Fisher for Cased Charge Blast Equivalence – I Ductile Casings," vol. 36, no. 4, pp. 310-313, 2011.
- [19] M. D. Hutchinson, "Replacing the Equations of Fano and Fisher for Cased Charge Blast Impulse-II-Fracture Strain Method," vol. 37, no. 5, pp. 605-608, 2012.
- [20] M. D. Hutchinson, "Replacing the Equations of Fano and Fisher for Cased Charge Blast Impulse – III – Yield Stress Method," vol. 39, no. 4, pp. 586-589, 2014.
- [21] B. Zecevic, J. Terzic, and A. Catovic, *Influence of warhead case material on natural fragmentation performances*. na, 2004.
- [22] G. Fairlie, "The numerical simulation of high explosives using AUTODYN-2D & 3D," in *Institute of Explosive Engineers 4th Biannual Symposium*, 1998, pp. 743-751.
- [23] C. E. Anderson JR, W. W. Predebon, and R. R. J. I. J. o. E. S. Karpp, "Computational modeling of explosive-filled cylinders," vol. 23, no. 12, pp. 1317-1330, 1985.
- [24] V. Gold, E. Baker, W. Poulos, and B. J. I. j. o. i. e. Fuchs, "PAFRAG modeling of explosive fragmentation munitions performance," vol. 33, no. 1-12, pp. 294-304, 2006.

- [25] X. Kong *et al.*, "A numerical investigation on explosive fragmentation of metal casing using Smoothed Particle Hydrodynamic method," vol. 51, pp. 729-741, 2013.
- [26] I. Cullis, P. Dunsmore, A. Harrison, I. Lewtas, and R. J. D. T. Townsley, "Numerical simulation of the natural fragmentation of explosively loaded thick walled cylinders," vol. 10, no. 2, pp. 198-210, 2014.
- [27] C. Woodford, "Iron and steel," 2018
- [28] R. Menikoff, "JWL equation of state," Los Alamos National Lab.(LANL), Los Alamos, NM (United States)2015.
- [29] J. Koehler and R. Meyer, "Explosives; ; Explosivstoffe," 1995.
- [30] X. Quan, N. Birnbaum, M. Cowler, B. Gerber, R. Clegg, and C. Hayhurst, "Numerical simulation of structural deformation under shock and impact loads using a coupled multi-solver approach," in *Proceedings of 5th Asia-Pacific Conference on Shock and Impact Loads on Structures*, 2003, pp. 12-14.
- [31] R. M. J. P. i. A. Lloyd, P. i. A. Aeronautics, and Aeronautics, "Conventional Warhead Systems Physics and Engineering Design, AIAA," vol. 179, 1998.
- [32] U. N. O. f. D. A. (UNODA), "The UN SaferGuard Programme , International Ammunition Technical Guidelines," 1998-2019.
- [33] W. F. Smith, J. Hashemi, and F. Presuel-Moreno, *Foundations of materials science and engineering*. Mcgraw-Hill Publishing, 2006.
- [34] J. R. Davis, *ASM specialty handbook: cast irons*. ASM international, 1996.